Friction
https://doi.org/10.1007/s40544-022-0609-6
ISSN 2223-7690
CN 10-1237/TH
REVIEW ARTICLE

Numerical micro-texture optimization for lubricated contacts—A critical discussion

Max MARIAN[1,*], Andreas ALMQVIST[2], Andreas ROSENKRANZ[3], Michel FILLON[4]

[1] *Department of Mechanical and Metallurgical Engineering, Pontificia Universidad Católica de Chile, Santiago 690411, Chile*

[2] *Division of Machine Elements, Luleå University of Technology, Luleå SE-971 87, Sweden*

[3] *Department of Chemical Engineering, Biotechnology and Materials, FCFM, University of Chile, Santiago 8370456, Chile*

[4] *Institut Pprime, CNRS, University of Poitiers, Poitiers Cedex TSA 41123, 86073, France*

Received: 04 December 2021 / Revised: 16 January 2022 / Accepted: 19 February 2022

Abstract: Despite numerous experimental and theoretical studies reported in the literature, surface micro-texturing to control friction and wear in lubricated tribo-contacts is still in the trial-and-error phase. The tribological behaviour and advantageous micro-texture geometries and arrangements largely depend on the contact type and the operating conditions. Industrial scale implementation is hampered by the complexity of numerical approaches. This substantiates the urgent need to numerically design and optimize micro-textures for specific conditions. Since these aspects have not been covered by other review articles yet, we aim at summarizing the existing state-of-the art regarding optimization strategies for micro-textures applied in hydrodynamically and elastohydrodynamically lubricated contacts. Our analysis demonstrates the great potential of optimization strategies to further tailor micro-textures with the overall aim to reduce friction and wear, thus contributing toward an improved energy efficiency and sustainability.

Keywords: micro-texturing; hydrodynamics; elastohydrodynamics; tribo-simulation; optimization

1 Introduction

As early as the mid-1960s, Hamilton et al. [1] verified an additional hydrodynamic pressure build-up by micrometre-scale irregularities on rotary shaft seals, thus enabling an additional load-carrying capacity. For face seals and thrust bearings, Anno et al. [2, 3] showed that surface textures can improve the resulting lubrication conditions. In commercial applications, stochastic textures were implemented early on by honing the cylinder liner raceways. Depending on the configuration and/or operating conditions, stochastic textures are capable of enhancing lubrication and serving as pockets to store lubricant and wear debris, even though this is conversely discussed in the literature [4, 5]. In the mid-1990s, surface texturing experienced a renaissance in magnetic storage devices [6] and mechanical seals under relatively extreme [7] due to the development of more efficient laser surface texturing (LST). Afterwards, tremendous research progress with numerous studies published has been made. The results of a comprehensive literature analysis including more than 1,400 Scopus-listed publications on surface texturing for tribological contacts in the past 30 years are summarized in Fig. 1. The procedure and Prisma flow chart for the systematic literature analysis are documented in the Appendix.

The dimensions of the surface textures considered can be assigned to the transition between the material microstructure and typical length scales in machine elements. Micro-textures are usually deeper compared with the roughness induced by finishing processes (fine turning, grinding, or polishing). Moreover, the lateral texture dimensions are at least one order of

*Corresponding author: Max MARIAN, E-mail: max.marian@ing.puc.cl

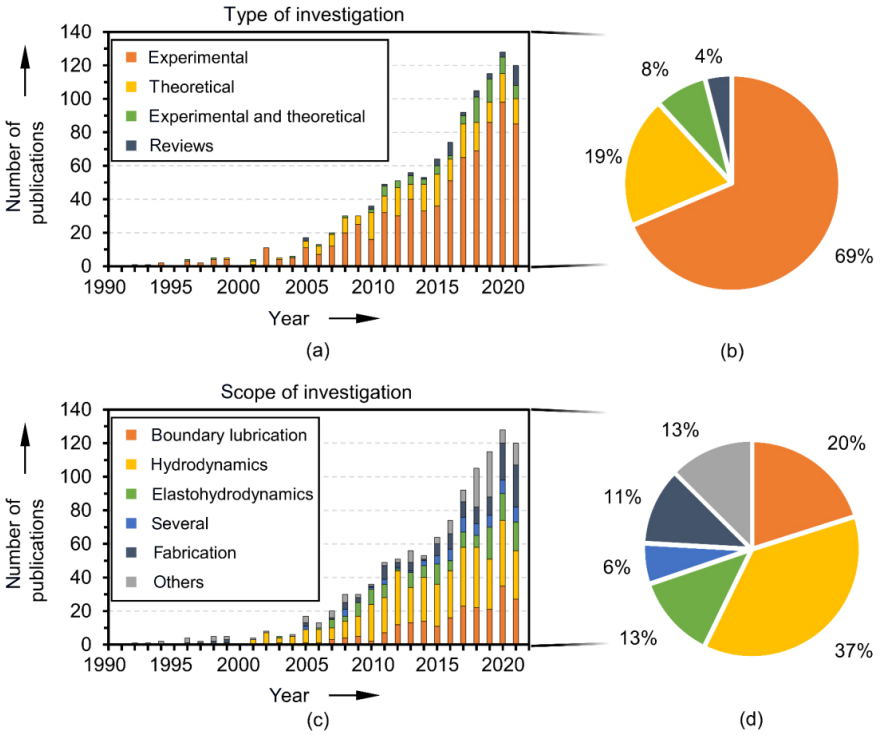

Fig. 1 Annual number of publications on surface texturing in tribology and classification by (a, b) type and (c, d) scope of investigations (as of December 2021).

magnitude larger than roughness features. The focus of this article is on discrete and geometrically well-defined micro-textures and not on directly influencing the surface topography in a stochastic way (roughness) [4] ("lower limit") nor on micro-cavities with depths and lengths/widths in the same order of magnitude [8] ("upper limit"), which frequently is incorrectly assigned to micro-texturing [9]. The publications were classified by the year of publication (Fig. 1(a)) and type of investigations into experimental, theoretical, combined, and review articles (Fig. 1(b)). Moreover, they were categorized by the scope of investigation according to the lubrication regime (Fig. 1(c) and 1(d)) into dry/boundary, hydrodynamic, elastohydrodynamic lubrication or several regimes (e.g., study of dry and lubricated contacts in one article). Within the scope of this article, the distinction between hydrodynamic lubrication (HL) and elastohydrodynamic lubrication (EHL) is based on the fundamental geometric and kinematic principles, while mixed lubrication or thermal effects may be involved in both. Thereby, HL refers to parallel, converging, or conformal contacts as found in thrust or journal bearings and explicitly includes potential load- or temperature-induced macro- elastic deformations. EHL relates to concentrated contacts with local elastic deformations in rolling bearings, gears, or cam-follower pairings. Most publications have been published in the last ten years, with a still increasing tendency each year. Experimental studies account for about 69% of the published articles, while 19% are based upon theoretical or numerical approaches and only 8% aim at combining numerical and experimental work. Furthermore, a large part of the studies deals with full-film HL, while significantly fewer studies address contacts in boundary lubrication or EHL. Only 6% include several types of contact conditions. Various comprehensive review articles from Gropper et al. [6] (HL contact modelling), Sudeep et al. [7] (concentrated contacts), Gachot et al. [10] (boundary, mixed, HL, and EHL), Rosenkranz et al. [11] (applied to machine elements), Grützmacher et al. [12] (multi-scale textures), Lu and Wood [13] (mechanical applications), Rosenkranz et al. [14] (synergetic effects with solid lubricants) as well as Allen and Raeymaekers [15] (hip implants) report the most important findings on surface textures in different tribological contacts/systems.

Regarding dry or boundary lubricated contacts,

surface textures improve friction and wear by reducing adhesion and the contact area as well as trapping wear debris. However, the influence on the tribological performance and the most beneficial texture geometry parameters strongly depend on the testing conditions, changes of the material microstructure, and surface chemistry during texturing [10, 14]. Consequently, textures can also increase friction or wear, and positive effects could hardly be demonstrated in higher category test methods (component or aggregate tests). Moreover, a reliable, theoretical design or even numerical optimization for surface textures under these conditions is yet to be developed.

Regarding lubricated conditions, there are numerous successful examples of the use of surface textures. Many experimental and numerical studies have been carried out on the effects of surface textures on the tribological behaviour under HL (Table 1). In this context, the governing effects regarding film formation and friction reduction are largely understood. The existing literature clearly shows that texture parameters must be designed mainly regarding the demands of the respective application. Experimental trial-and-error effort can be greatly reduced by using robust simulation models. These models have been developed comparatively far but are relatively complex due to the numerical challenges and the included phenomena, such as cavitation, thermal and non-Newtonian effects, solid asperity contact, and elastic deformation. The lack of commercial solutions or detailed recommendations for the implementation of contact simulation and texture optimization makes it difficult to implement them in an industrial context.

The use of surface textures in EHL has been discussed more controversially in the literature, and the underlying mechanisms are yet to be fully explored. The investigations carried out are summarized in Table 2. Surface texturing helps to increase the lubricant film under certain circumstances, resulting in potential friction savings. Like HL, the geometric texture parameters must be designed for the demands of the respective application. The low number of successful, application-oriented investigations and the high proportion of trial-and-error studies using basic laboratory test-rigs relate to the lack of suitable and available approaches for simulating these complex contacts, which holds especially true for mixed lubrication.

Despite numerous experimental and numerical studies for HL and EHL contacts, surface texturing still largely relies on trial-and-error testing. Although some general design recommendations have been

Table 1 Overview of relevant studies conducted for HL contacts summarizing the observed effects and beneficial micro-textures.

Contact geometry	Parallel [16–70]	
	Converging [71–77]	
	Conformal [78–88]	
Lubrication conditions	Full film [16–20, 23–27, 29–60, 62, 63, 66–71, 73–89]	
	Mixed lubrication [22, 28, 44, 52–65, 84]	
Test category	Model test [28, 29, 55–59, 72, 89]	
	Specimen test [25–27, 31, 36, 44, 50–52, 69]	
	Component test	Mechanical seals [17–20, 70]
		Cylinder liner [62–65]
		Thrust bearings [23–27, 30–36, 40–44, 47, 48, 68, 69]
		Journal bearings [84–88]
	Aggregate test [54]	
Main effects	Friction reduction [16–19, 28, 31–33, 46, 50–52, 58–63, 68, 69, 78, 79, 84]	
	Increasing the load-carrying capacity [20, 23, 24, 26, 27, 30, 31, 35, 46, 66, 68, 69, 75, 76, 88–90]	
	Enlargement of lubricant gap [57–60]	
	A shift of the Stribeck curve [44, 84]	
	Friction increase [21, 58–60, 78, 79, 90]	
Beneficial micro-textures	Closed geometries	Dimples [17–20, 31, 35–38, 50–54, 66, 67, 89–91]
		Chevrons [49, 61, 64, 65, 68, 70, 90]
		Grooves [75, 76, 90]
	Orientation	Perpendicular to sliding direction [45–48, 75, 76, 90]
	Texture density	10%–100% (pocket) [4, 10, 17, 34, 35, 44, 66, 90–93]
	Texture length	40%–90% [35]
	Texture width	70%–90% of bearing width [35, 90, 94]
	Texture depth	6%–10% of the texture width [10, 18, 55, 90, 93]
		40%–80% of film height [6, 32–34, 37, 38]

Table 2 Overview of relevant studies conducted for EHL contacts, observed effects, and beneficial micro-textures.

Contact geometry	Concentrated [95–140]	
	Conformal [141–152]	
Contact form	Point contact [95–105, 107–118, 131, 133, 138–140]	
	Elliptical contact [124, 127]	
	Line contact [106, 119–123, 126, 128–130, 134–137, 140]	
Kinematics	Sliding	Continuous [95–100, 112, 116, 118]
		Reciprocal [111, 113–115, 117, 133]
	Rolling	Continuous [95–100, 103, 106, 120]
	Sliding–rolling	Continuous [95–103, 105–108, 126, 134, 135, 137–140]
		Reciprocal [108, 109]
Lubrication conditions	Full film [95–100, 107, 108, 111, 119–122, 126, 127, 136]	
	Mixed lubrication [101–106, 109, 111–118, 123, 125, 126, 128, 129, 133–135, 137, 140, 150]	
Test category	Model test [95–109, 111–121, 123, 125, 131, 133, 138–140]	
	Specimen test [149]	
	Component test	Rolling bearings [128, 153]
		Gears [123, 130]
		Cam/tappet contacts [126, 134, 135, 137, 140]
		Rotary shaft seals [145, 146]
		Hip implants [140, 147, 152]
	Aggregate test [129]	
Main effects	Enlargement of lubricant gap [99–103, 105–110, 125, 126, 140]	
	Deterioration of lubricant gap [95–98, 101–103, 106–109, 124, 126]	
	Friction reduction [107, 108, 111, 112, 116–118, 121, 123, 125, 126, 131, 133–135, 137, 138, 140, 147, 148]	
	Friction increase [121, 123, 140]	
	Wear increase [118, 134]	
Beneficial micro-textures	Closed geometries	Dimples [99–103, 105–109, 133, 134, 138, 140, 141]
		Grooves [107, 108, 111, 126, 129, 135]
	Orientation	Perpendicular to sliding direction [107, 126, 127, 134, 135, 137, 140]
	Texture density	10%–20% [112, 116, 126]
	Texture width	< contact area [107, 112, 133, 140]
	Texture depth	< 10 μm [99, 100, 116, 133, 140, 154]

derived in literature, their introduction into industrial applications is hampered by the fact that the tribological performance mostly depends on the respective contact and operating conditions. Therefore, surface textures always must be designed for the underlying kinematics, stresses, and contact situations. Suitable simulation approaches can serve as a numerical zoom into the tribological contact, thus contributing toward the design of surface textures with reduced experimental effort. However, the requirements for numerical modelling are complex due to the involved physical phenomena and multi-scale domains. Consequently, the practical feasibility in an industrial context has been hampered by the lack of publicly available source codes, commercial software solutions and/or detailed recommendations for the consideration of relevant phenomena as well as the lack of a methodology for efficient optimization. These aspects, with a strong focus on numerical modelling of both HL and EHL contacts, as well as the involved optimization approaches have not yet been addressed by other articles reviewing the state-of-the-art in surface micro-texturing. Therefore, this article aims at shedding some light on numerical modelling and optimization approaches. Numerical fundamentals required to simulate and optimize micro-textured HL and EHL contacts will be introduced in Section 2. Subsequently, the underlying mechanisms and influences of micro-textures in various parallel or convergent/conformal HL, as well as hard and soft EHL applications, are critically discussed in Section 3. Finally, current challenges and future research directions are derived in Section 4.

2 Modelling and simulation in lubrication

This section presents a short introduction of the general numerical background for modelling HL (Section 2.1) and EHL (Section 2.2) contacts as well as optimization strategies (Section 2.3).

2.1 Modelling of textured HL contacts

By combining the Navier–Stokes equations with thermodynamic state equations and thermal energy conservation, the flow in HL contacts can be simulated using purpose-built solvers or commercial computational

fluid dynamics (CFD) software. However, this still requires comparatively high and time-consuming computational efforts, especially for textured contacts due to the required fine meshing, possible time-dependent effects, and numerical instability. With assumptions and simplifications, it is possible to derive differential equations that can be solved with less computational effort while maintaining sufficient accuracy for thin-film lubrication problems. The Reynolds equation was originally derived assuming that the lubricant is incompressible and iso-viscous [155], while the ratio of the gap height to lateral contact dimensions is vanishingly small. Constraints regarding incompressible and Newtonian fluids were not necessary since a derivation from the compressible Navier–Stokes equations and the compressible continuity equation while considering Newtonian or non-Newtonian fluids was later shown to be possible. Variants of the generalized Reynolds equation were presented by Dowson [156] for Newtonian fluids or Najji et al. [157] (isothermal) or Yang and Wen [158] (thermal) for non-Newtonian fluids. Some of the remaining assumptions, however, have different implications regarding the applicability of the Reynolds equation at larger Reynolds numbers (*Re*), for which the texture height (h_t) to length (l_t) (in direction of motion) ratio is not sufficiently small to be neglected. There are many studies verifying the importance of including the terms in the Navier–Stokes equations governing inertia. Arghir et al. [9] and Sahlin et al. [159] showed that the inertia-based contributions in the Navier–Stokes equations (not present in the Reynolds equation) generate a net pressure build-up and load-carrying capacity for parallel surfaces with a single macro-cavity. Despite Dobrica and Fillon [8] obtained a similar tendency for the first dimple, they showed that the inertia effects decrease the pressure for the following ones in the partially textured zone, thus reducing the maximum pressure and the pressure in the non-textured zone. The main result was that the inertia effects decrease the load-carrying capacity in partially textured sliding bearings. However, for sufficiently small *Re* as well as for small ratios of texture height to length, i.e. $(h_t/l_t)^2 << 1$, a rather small error can be expected [160, 161]. This was supported by studies presented from Van Odyck and Venner [162] as well as Wen et al. [163]. As pointed out by Feldman et al. [164], the Reynolds equation can be considered a conservative estimation even in case of unfavourable texture dimensions. Therefore, Etsion [165]–despite not providing verifiable evidence–rated the accuracy of the Reynolds equation as sufficient for typical micro-textures generated by LST.

For numerical flow simulations, either the whole contact area of the respective application can be solved, or mirror and rotational symmetry can be utilized to simplify and reduce the problem to cells with periodic boundary conditions. The computational domain is discretized into a finite number of sub-regions or volumes. The finite difference method (FDM) solves the equations in differential form, while the support points are located at the corners of the volume elements. The finite volume method (FVM) establishes solutions of the sought variables by integration of the differential equations at the centres of the control volumes. Both methods are well suited for the simulation of HL contacts. Moreover, the finite element method (FEM) can be used, where the basic idea is to fit the solution for the nodal points of the finite elements to mathematical shape functions, thus generating a piecewise composite approximation of the overall solution.

The first numerical solution of the Reynolds equation goes back to Sommerfeld [166], who employed trigonometric substitution without the consideration of cavitation. This results in a point-symmetric pressure profile, and the maximum positive pressure corresponds to the minimum negative pressure. However, the lubricant film ruptures due to the limited ability to transmit tensile stresses and gas or vapour bubbles are formed (cavitation). This results in a two-phase flow of lubricant and gas or vapour in the cavitation area. Various numerical approaches have been developed for the numerical consideration of cavitation (Table 3). Non-mass conserving models lead to a discontinuity at the transition between the pressure and cavitation regions and contradict the continuity equation (conservation of mass). Despite errors in the computational results due to the violation of the continuity equation at film cavitation and reformation [167], non-mass-conserving cavitation models are widely used in the literature due to their

Table 3 Overview of the established cavitation models.

Category	Approach	Characteristics	Ref.
Non-mass-conserving	Gümbel/half-Sommerfeld solution	Setting negative pressures to zero.	[170]
	Swift–Stieber/Reynolds boundary condition	Setting negative pressures to zero and ensures zero pressure gradient at the transition from pressure to cavitation region.	[171–173]
	Gauss–Seidel iteration	Iterative calculation of the location of the cavitation region. Setting negative pressures to zero during the calculation. Applicable to FDM.	[174]
	Murty algorithm/penalty method	Setting negative pressures to zero during the calculation by a penalty term added to the Reynolds equation. Applicable to FEM.	[175, 176]
Mass-conserving	Jacobson, Floberg, Olsson (JFO) boundary condition	Consideration of fluid transport between the resulting gas and vapour bubbles as well as fluid film reformation. Numerically complex dynamic boundary conditions.	[177–179]
	Elrod algorithm	Switch function to consider the cavitated phase as compressible based on the pressure–density relation with constant bulk modulus. Applicable to FDM and FVM. Later extended to account for compressible lubricant in liquid and cavitated phase.	[180–184]
	Complementarity-based methods	Generalized complementarity problem formulation of the switch-function-based approaches. Applicable to FDM and FEM. Later extended to account for compressible fluids and EHL conjunctions	[185–188]
	Variational inequality	Variational inequality formulation. Applicable to FEM.	[169, 189–191]

comparatively simple implementation [168]. However, a cavitation algorithm applicable to study hydrodynamic flows between textured surfaces must be mass-conserving to obtain reliable predictions [6, 23, 169].

The solution of the Reynolds equation requires knowledge of the lubricant film height (distance between both surfaces). The lubricant gap equation is thus composed of the rigid distance between the undeformed bodies, their macroscopic geometries, the surface topography on different scales, and possible elastic or elasto-plastic deformations. Load-independent relationships can be formulated for the undeformed macro- and micro-geometry. The hydrodynamic pressure development in lubricated contacts is substantially influenced by the micro-geometry. Depending on the characteristics and structure of the surface topography, the macro-hydrodynamic pressure development can be reduced or increased. These micro-hydrodynamic influences can be considered in a direct (deterministic) or indirect (stochastic) way. For the deterministic coupling of micro- and macro-hydrodynamics, the surface topography is mathematically described in the lubricant gap equation. This requires fine meshing, which is associated with long computation times. Therefore, indirect coupling based on stochastic approaches and an averaged form of the Reynolds equation has been developed [192, 193]. Using flow factors according to Patir and Cheng [194, 195], the mean volume flow between two rough surfaces in a control volume is balanced directionally for a given mean gap height with defined boundary conditions. Flow factors for the pressure flow and the shear flow describe the difference between rough and smooth gaps, thus being included in the Poiseuille and Couette terms of the Reynolds equation, respectively. For engineering surfaces, a distinction can be made between two micro-geometric scales. On the one hand, this is the roughness determined by machining processes, which can be stochastic, irregular, or partially directional. On the other hand, there are discrete and intentionally produced surface textures, which are one or more orders of magnitude larger in depth as well as lateral dimensions than typical roughness features. Flow factors and homogenization approaches may also be used to efficiently investigate contacts with discrete textures [196–208]. However, larger deviations are expected due to the validity only for nominally constant (parallel) lubricant film heights and larger lateral dimensions of the texture elements. Therefore, a semi-deterministic approach is advisable, which deterministically considers the micro-textures while the surface roughness, if necessary,

is stochastically considered [12, 209]. Depending on whether the micro-textures are quasi-stationary in the contact area, or whether they move through it in a time-transient manner, and whether there are non-stationary operating conditions, time-dependent squeeze effects can be neglected or need to be considered [210]. For HL contacts, however, texturing the stationary surface can yield better results than texturing moving parts [39].

For mixed lubrication, there is a superposition of the hydrodynamic [194, 195] and solid–solid asperity due to contacting surface roughness. For the determination of the real contact area and the pressures, different approaches can be coupled directly (deterministically) or indirectly (stochastically) with hydrodynamic approaches. Regarding latter, the load-carrying capacity of the surface roughness can be incorporated as a function of the mean fluid film height by integral solid asperity contact pressure curves. For given surface pairings, these can be calculated with simple models assuming idealized roughness geometries and statistical averaging. An analytically solvable approach to estimate the carried load between an elastic rough surface and a rigid smooth plane based on the deformation of asperities following the Hertzian theory was proposed by Greenwood and Williamson [211]. This was extended by the consideration of curved surfaces [212], elliptic parabolic asperities [213], anisotropic surfaces [214], and two rough surfaces [215]. Various authors developed analytically solvable approaches to account for elastic, elasto-plastic, or plastic material properties [216–219]. Furthermore, there are more complex models based on the elastic half-space theory or FEM [220–229], which allow for the consideration of three-dimensional (3D) contact conditions, deformative interactions, elasto-plastic effects, and real (measured) surfaces.

Frictional heating due to the internal shear resistance of the lubricant or solid asperity contact leads to the formation of temperature distributions. The calculation of the temperature distribution in the lubricant is based on the energy conservation and the first law of thermodynamics for an open system. By neglecting thermal radiation, chemical reactions, gravity, and anisotropic thermal fluid properties, the heat equilibrium can be determined by calculating the heat conduction and convection in the lubricant gap as well as in the contacting bodies with heat sources for lubricant compression/expansion and shearing [230]. For mixed lubrication, these heat sources also arise from contacting asperities (flash temperatures). Since convection does not occur in solids, the energy balance at the volume element is based on the first law of thermodynamics for a closed system [230]. By simplifying and neglecting temperature- and pressure-dependent density changes of the solid, the Fourier's differential equation of the transient heat conduction can be obtained [230]. The latter can be solved numerically or analytically [231–235] by means of a Laplace transformation [230].

Despite the parallel or conformal contact geometry, higher external and inertial forces as well as hydrodynamic pressures and temperatures lead to macro-deformations, which directly influence the geometry of the lubricant gap and the pressure development [230]. Although being often referred to as EHL, we assign these contacts to HL in this contribution. The coupling between the lubricant's hydrodynamics and the calculation of the deformation can be done in a quasi-static or dynamic way. Regarding quasi-static calculations, the hydrodynamics can be coupled directly with FEM models or elastic half-space approaches [230]. Besides that, a compliance (influence number) matrix can be derived from a one-time FEM simulation during pre-processing. Subsequently, the HL simulation is coupled with the compliance matrix to determine the purely linear-elastic deformation at each node [230]. If influences due to inertia of moving components on the gap deformation must be considered, hydrodynamics and deformation need to be coupled dynamically. This is usually done within elastic multibody simulations (MBS), in which the Newton's equation of motion is solved. In this regard, each component can be represented by a full FEM model. However, this usually involves high computational costs due to the required time integration and the large number of degrees of freedom [230]. Therefore, reduction methods provide higher efficiency by extracting the essential information on the deformation behaviour from the FEM as well as the dominating inherent frequencies or mode shapes (eigenmodes) [236]. For untextured HL contacts such as thrust slider bearings, mechanical and thermal deformations

may even contribute to the load-carrying capacity [237]. Regarding micro-textured HL contacts, Chalkiopoulos et al. [238] reported that mechanically and thermally induced deformations led to a substantial alteration of the fluid film geometry in thrust pad bearings, while generating a converging and a diverging region in flow direction. This reduced the hydrodynamic effect of the textures, thus diminishing the load-carrying capacity and increasing the frictional torque. Similarly, Henry et al. [44] experimentally observed that temperature gradients led to an expansion of the pads, which favoured a convergent gap zone at the leading edge and a diverging gap at the pad's end. Consequently, the hydrodynamic pressure build-up effect of the textures became insignificant compared to that of the convergent gap. In this sense, the potential influence of mechanical and thermal deformations should be considered when designing micro-textures for HL contacts.

2.2 Modelling of textured EHL contacts

EHL contacts are characterized by the lubricant's hydrodynamics and elastic deformations of the contacting bodies. Coupled solutions with an equilibrium of forces (load balance) including fluid and solid domains are required (fluid-structure interaction (FSI) to be considered). CFD approaches such as those in Refs. [239–241] do not allow for an efficient solution of micro-textured EHL contacts, since the mostly prevailing rolling–sliding conditions with micro-textures traveling through the contact area require the consideration of time-transient effects. Therefore, the modelling of hydrodynamics is usually based on the Reynolds equation. Like HL contacts, the consideration of micro-textures in EHL contacts leads to a violation of the assumptions in the derivation of the Reynolds equation. However, Almqvist et al. [242] showed that small ratios of amplitude to wavelength of a single elevation (essentially the opposite of a micro-texture) led to only small deviations under EHL conditions. Due to the higher viscosity and thinner fluid film as well as the resulting low *Re* in combination with the typically flat micro-texture geometry, Reynolds-based approaches can be considered as appropriate. Therefore, the extra computational cost associated with CFD does not justify the use as a replacement to the much less computationally demanding Reynolds-based approaches. Considering weak coupling, the hydrodynamic pressure and the elastic deformation are sequentially/iteratively solved until a defined convergence criterion is reached. Initial solutions of the EHL problem were based on the inverse method, for which the Reynolds equation is solved for the lubricant gap at the given pressure [243–245]. In contrast, the direct method solves the differential form of the Reynolds equation for the pressure at a given lubricant film height [246–249]. Based on the leading work of Lubrecht and Venner using FDM for hydrodynamics and an elastic half-space approach for the elastic deformation in conjunction with multigrid (MG) [250] and multilevel multi-integration (MLMI) methods [251, 252] as well as suitable relaxation methods [253], this is still the most widely used approach to solve the EHL problem. Even under severe conditions, the solution convergence and stability could be further improved by a fast Fourier transformation (FFT) solution of the half-space contact mechanics [254–257]. This is contrasted to the strong coupling of hydrodynamics and elastic deformation, which are numerically based on a Newton method [258–260]. However, the use of a half-space approach results in a fully occupied matrix in the system of equations to be solved, which leads to high computational effort and memory requirements. Ultimately, Habchi et al. [261] suggested a FEM formulation for the elastic deformation and the discretization of the Reynolds equation by an FEM approach to obtain a sparse matrix. This leads to a good convergence behaviour and enables the use of commercial software solvers [262–264].

Due to the characteristic behaviour of the EHL contact and the complex numerical formulation along the necessity to solve the energy equations across the fluid film, the thermal influence has been given limited attention. For isothermal cases, the differences between non- and mass-conserving cavitation models are marginal [136]. For higher loaded EHL contacts with elevated sliding velocities and/or substantial slip, shear-thinning and thermal effects may significantly influence the lubrication behaviour. Generally, non-Newtonian and thermal effects due to lubricant shearing and compression moderately affect the film thickness

since the latter is largely driven through the fluid viscosity at the contact inlet. However, the fluid traction can be notably influenced. Furthermore, the lubricant film thickness can be overestimated when solved by non-mass-conserving cavitation models [265]. Numerically, the isothermal EHL and thermal problem are commonly solved separately and an iterative procedure weakly couples their solution until reaching convergence [263, 266, 267]. Usually, this is associated with a loss of information and slower solution compared to fully coupled approaches [264]. Regarding micro-textured EHL contacts, Weschta [126] and Tremmel et al. [268] studied the influence of shear-thinning and thermal effects by applying a generalized Reynolds equation, which was strongly and weakly coupled with the elastic deformation and the thermal equations, respectively [158]. It was shown that there is a shift of the lubrication gap level to smaller values and a damping of the textured-induced pressure peaks due to lowered viscosities compared to an isothermal and Newtonian calculation.

Similar to HL contacts, mixed lubrication and the load-carrying proportion due to solid asperity contact can be treated deterministically [256, 269, 270] or stochastically [271–277]. Since micro-textures in full-film EHL contacts tend to increase the fluid traction [135] and positive effects can be rather expected in mixed lubrication, the consideration of solid asperity effects is crucial [140].

2.3 Micro-texture parametrization and optimization strategies

Numerical work to study the influence and design of micro-textures is based on a variation of geometric parameters. The design space depends to some extent on the fabrication processes. Following Costa and Hutchings [278], these can be categorized in chemical [279–282] or physical [283–289] addition, thermal [290–296], chemical etching [297–301], mechanical [302–305] removal or movement (direct laser interference patterning [306–309], and forming [137, 310–314]) of material. All processes have in common that they have been adapted or newly developed for the fabrication of discrete micro-texture elements. A comparison of the design possibilities in terms of texture and component surface as well as materials of various processes frequently employed in the field of tribology is shown in Table 4. The realization of a successful industrial implementation also depends on the possibility to implement a cost-efficient texturing, in already optimized production chains. The geometric resolution and production speed are frequently found to oppose each other, with the advantages of single-step processes prevailing from an economic point of view. In case of material-removing processes (laser texturing or micro-milling), the required process time tends to increase with the textured area. The advantages of material-moving processes are particularly beneficial with respect to the high variability, high throughput, design freedom, and accuracy of laser interference texturing or micro-coining.

For simulation and optimization, the depth profile of the micro-textures must be described in the lubricant gap equation by means of a parametrized mathematical formulation. As illustrated in Fig. 2, different base and

Table 4 Overview of the possibilities and limitations of various micro-texturing processes in extension to Ref. [278].

		LST	Chemical etching with masking	Chemical etching without masking	Laser interference texturing	Micro-coining
Geometrical resolution	Lateral	> 5 µm	> 20 µm	> 150 µm	> 1 µm	> 5 µm
	Depth	> 1 µm	> 2 µm	> 5 µm	> 1 µm	> 1 µm
Component surface	Flat	✓	✓	✓	✓	✓
	Curved	✓	✓	✓	✓	✓
	Cylindric	✓	✓	✗	✓	✓
Component material	Metals	✓	✓	✓	✓	✓
	Ceramics	✓	✓	✓	✓	✗
	Polymers	✓	✗	✗	✓	✓

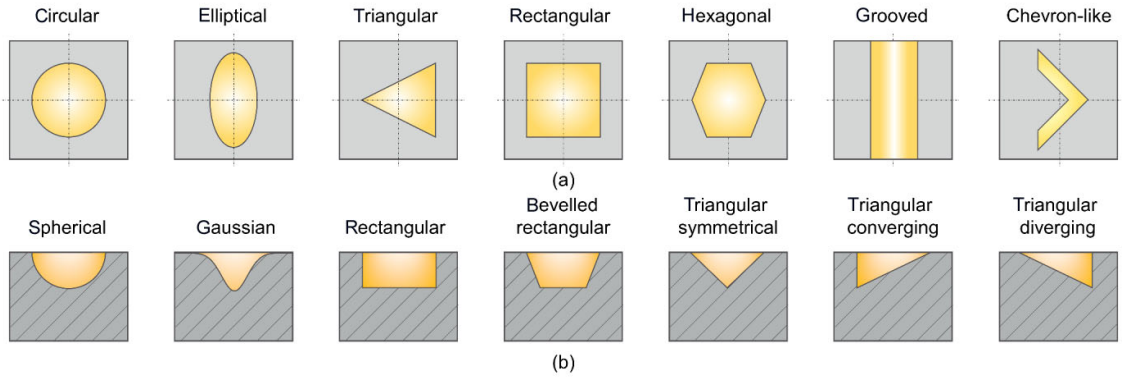

Fig. 2 Selection of different (a) micro-texture base shapes and (b) bottom profiles. Reproduced with permission from Ref. [6], © The Authors 2015.

bottom shapes are conceivable. Although circular and rectangular or grooved textures with spherical or flat bottom shapes represent the most studied geometries so far, today's manufacturing techniques are capable of fabricating all kinds of complex textures and texture combinations [8]. Apart from the base shape and bottom profile, individual textures are characterized by their lateral dimensions and depth as well as orientation with respect to the sliding direction. Texture patterns are described by the overall extension and position of the textured area as well as the lateral/circumferential distances or angular/radial offset between the individual texture elements. In many studies, the aspect ratio, texture density and relative texture depth are given to describe the used texture. As pointed out by Etsion [165], it is essential that the different texture geometries and patterns are optimized separately before deriving optima from all geometric variations since it is not meaningful to compare different base geometries with similar dimensions.

Beneficial combinations of texture parameters have been mostly identified based upon "simple" parameter studies. Partially, this is accomplished by means of a statistical design of experiments (DoEs) to ensure sufficient significance with minimum computational effort. The most basic form relates to full factorial DoEs, for which all the possible discrete combinations of the considered input variables (factors) are tested. With alternative forms, e.g. partial factorial designs, central composite designs (CCD), or Box-Behnken designs, the increase of the necessary number of simulations with the rising number of factors can be kept comparatively low while maintaining a good predictive capability [315].

In considerably fewer studies on micro-textures, numerical optimization algorithms were employed. This can be done directly [49], i.e., based entirely on HL or EHL tribo-simulations, or indirectly by surrogate, approximation, or meta-models [316, 317]. Meta-models range from simple linear or quadratic regressions to more complex approaches such as polynomial regression, moving least squares (MLS), or Gaussian process regression (GPR) as well as methods of machine learning (ML) or artificial intelligence (AI) approaches, such as support vector machines (SVM) or artificial neural networks (ANNs) [318, 319]. Thereby, experimental designs adapted to the properties of the numerical simulation and statistical modelling can be used. To generate a broad spectrum of approximation or meta-models, a so-called Latin hypercube design (LHD) or Latin hypercube sampling (LHS) from the group of equally distributed test fields is particularly suitable [315, 320]. The test data are distributed to fill the factor space as evenly as possible and provide information about almost every area with little computational effort [321]. Suitable algorithms based on tribo-simulations or meta-models can then be used to determine the global optimum of geometric micro-texture parameters with respect to the objectives relevant for the respective application. In principle, gradient-based [322], response surface [323, 324], and nature-inspired methods such as particle swarm optimization (PSO) [325] or evolutionary/genetic algorithms (EA/GA) [326, 327] can be employed for this purpose. The latter usually represents an efficient

and flexible way to optimize an unknown problem. The sequential quadratic programming (SQP) method is another efficient approach for constraint non-linear optimization problems [322, 328, 329]. Furthermore, topology optimization [330] is of interest in the context of tailoring the topography of tribo-contacts. This involves the optimization of material layout within a given design space, for a given boundary conditions and constraints. The design is optimized with respect to the system performance using either gradient-based mathematical programming techniques such as the optimality criteria algorithm and the method of moving asymptotes [331, 332] or non-gradient-based algorithms such as EA. The advantage lies in the geometric versatility exceeding the design freedom of conventional parametric approaches.

3 Micro-texture mechanisms and optimization

This section presents a detailed overview and critical discussion of the insights deduced from numerical modelling and optimization for HL (Section 3.1) and EHL (Section 3.2) contacts.

3.1 HL contacts

A prerequisite for the hydrodynamic pressure build-up and separation of relatively moving surfaces in the presence of a lubricant is a converging fluid film gap. The distribution of the hydrodynamic pressure as well as the cavitated region for a parabolic slider geometry is exemplarily illustrated in Fig. 3(a)). The results for an infinite two-dimensional (2D) slider bearing (velocity u = 1 m/s, isoviscous fluid viscosity η = 0.01 Pa·s) presented in Fig. 3 were calculated based upon FDM by means of a pivoting algorithm that solved a linear complementary problem (LCP) formulation of the Reynolds equation in a mass-conserving way [185, 333]. In plain bearings, the pressure build-up is typically realized by a tilt (Fig. 3(b)) or step (Fig. 3(c)) in one of the surfaces. At the trailing edge, pockets or micro-textures can also act as a converging wedge or step and thus as a local hydrodynamic bearing. As pressure increases in the converging region, it theoretically decreases to the same extent in the diverging region. However, negative pressures are limited by the restricted possibilities of the lubricant to transmit tensile stresses and resulting

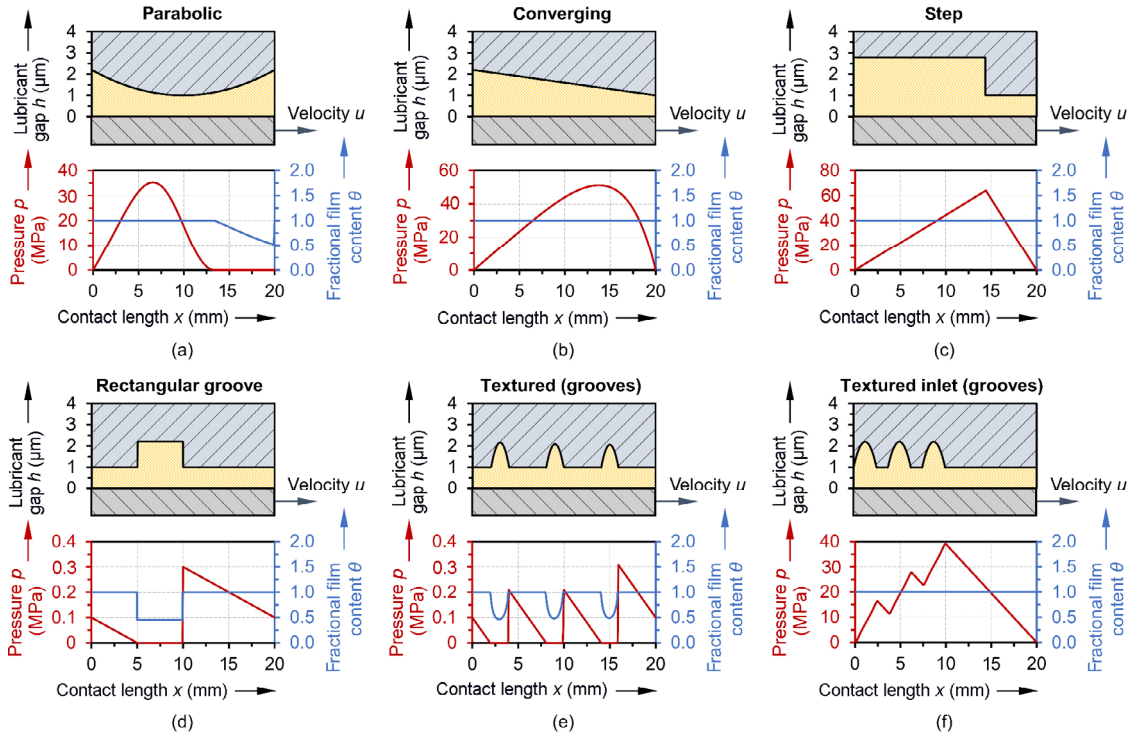

Fig. 3 Exemplary lubricant gap, pressure, and fractional film content distribution in a 2D HL contact with (a) a parabolic or (b) converging geometry, (c) a step, (d) a pocket as well as (e) several micro-textures that are equally distributed, or (f) concentrated to the contact inlet.

cavitation [25, 334]. This yields asymmetric pressure profiles [16] (Fig. 3(d)), and the negative pressure in the cavitation region can additionally lead to inlet-suction of lubricant [335, 336]. However, if the pressure gradient is not sufficiently high, e.g. the supply pressure and cavitation pressure are equal, there will be an insufficient lubricant supply to the texture and no sufficient pressure build-up. If the supply pressure is too high, no cavitation occurs, and the pressure decrease compensates for the pressure increase [8]. Through a suitable design of one or more micro-textures (Figs. 3(d) and 3(f)), the positive aspects (hydrodynamic pressure build-up) may balance or even outweigh the negative effects (cavitation effects and pressure drop). Thus, a substantial load-carrying capacity can be attained even in a nominally parallel lubricant gap [337]. In addition, micro-textures can shift the Stribeck curve toward lower film heights [19] and under mixed lubrication, and serve as a lubricant reservoir as well as trap wear particles [17, 91]. These effects are complex and partly superimposed phenomena, which strongly depend on the respective contact situation and the dimensions of the test set-up or application. Hence, in the following, the research on the influence of micro-textures and the optimization of geometrical parameters in HL contacts will be discussed structured by the tribological system.

3.1.1 Parallel HL contacts

(1) Mechanical seals

Pioneering work in the field of textured tribological systems with parallel surfaces goes back to the studies on mechanical seals from Etsion et al. In several Reynolds-based studies on cup-shaped textures, a significant enhancement of the sealing behaviour, service life, and friction performance was verified [16, 17]. Parametric studies revealed a smaller influence of the texture geometry, but a dependency on the aspect ratio and the area coverage was verified [19]. Both parameters need to be optimized for the respective operating conditions, and the area coverage should be below 20% [91]. Furthermore, it was shown that partial instead of full texturing is more advantageous [18]. In numerical investigations using a mass-conserving cavitation model, Meng et al. [21] verified an improved sealing behaviour, while only partially demonstrating an improved load-carrying capacity for micro-textured surfaces. Brunetière and Tournerie [22] simulated textured sealing surfaces using the Reynolds equation with a mass-conserving cavitation and a deterministic mixed lubrication model. It was shown that textures only led to the formation of a load-carrying capacity when surface roughness was considered. For ideally smooth surfaces with surface textures, no beneficial effects regarding load-carrying capacity were verified. This is contradictory to most previous theoretical investigations and can be attributed in particular to the use of the mass-conserving cavitation model [168]. Wang et al. [70] solved the two-dimensional Reynolds equation for the conditions of rotational gas face seals and applied an non-dominate sorting genetic algorithm (NSGA) for Pareto-optimizing the micro-texture geometry to simultaneously maximize the load-carrying capacity while minimizing leakage. Thereby, asymmetric V-shaped textures were found to be superior to regular shapes (circle, ellipse, square, and triangle), especially under high-speed conditions.

(2) Parallel thrust bearings

Qiu and Khonsari [23–25] numerically and experimentally showed for fully textured rotating thrust bearings that a non-mass-conserving consideration of cavitation leads to an overestimation of the load-carrying capacity. Additionally, they verified that the formation of the cavitation region depended on the rotational speed. By properly designing the aspect ratio and area coverage for the respective sliding speed, friction was reduced, which aligns well [26, 27]. Zhang et al. [28] demonstrated improved friction for laboratory experiments with textured disks in contact with a flat pin under mixed lubrication. By numerical calculations based on the Reynolds equation with flow factors, a mass-conserving cavitation model, and a stochastic asperity contact model, they revealed fluctuations in the calculated friction, which was attributed to the alternating sliding over of areas with higher and lower pressures. Codrignani et al. [89] applied the adjoint optimization technique (Fig. 4(a)) to determine optimal surface topographies in a crowned pin-on-disk setup by solving the Reynolds equation with a mass-conserving cavitation model. Although considering a concentrated contact, elastic deformations

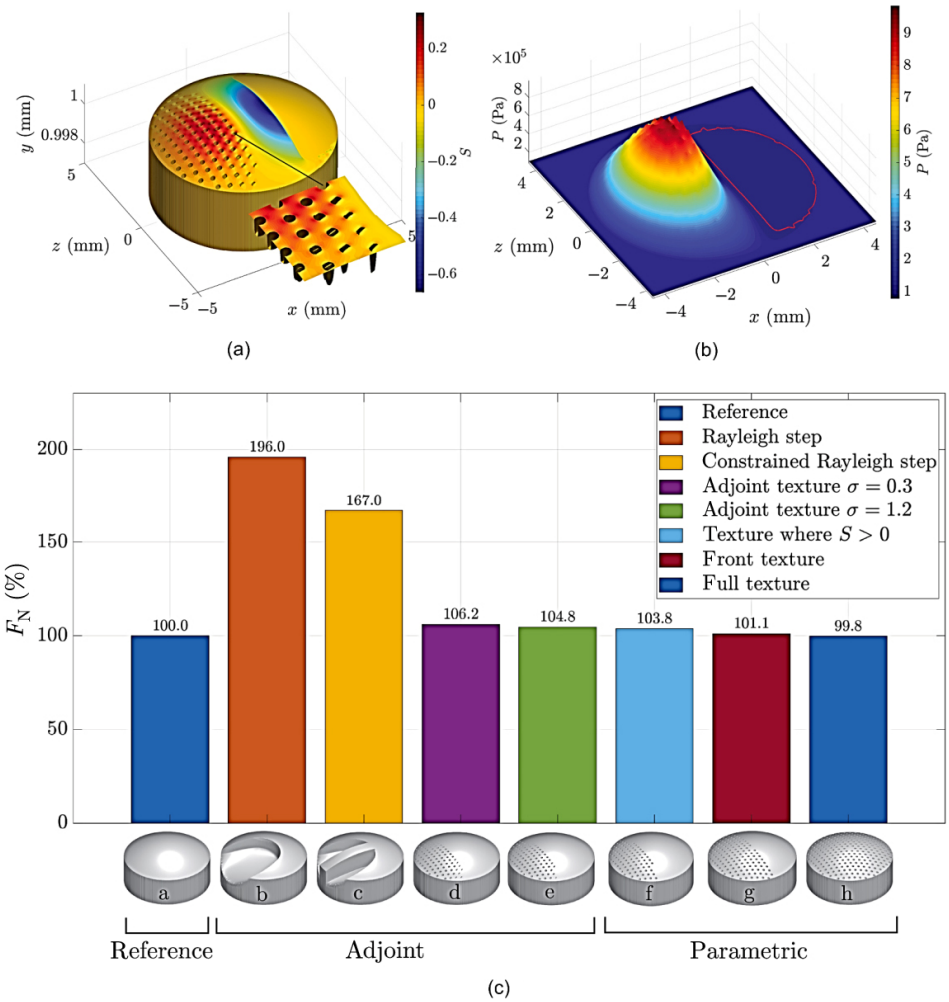

Fig. 4 (a) Optimized textures and sensitivity of the pin surface and (b) resulting pressure (P). (c) Comparison of the load-carrying capacity (F_N) of the reference and optimized textures by parametric studies and the adjoint method. Reproduced with permission from Ref. [89], © The Authors 2020.

were neglected. This optimization approach tailored the entire gap height distribution point by point, thus enabling a free-form optimization in a more efficient way than traditional optimization approaches and parametric studies. It was reported that the traditional approach to texture the full front of the pin did not lead to an ideal increase in load-carrying capacity. Instead, it was beneficial to texture only part of the front portion of the pin (Figs. 4(b) and 4(c)). Optimizations were further conducted as a function of operating conditions, indicating a linear relationship between the gap height and optimal texture depth. However, for the chosen operating parameters and geometry, the absolute improvement in load-carrying capacity was fairly small compared to a Rayleigh step bearing irrespective of the optimization techniques (Fig. 4(c)).

Numerical studies performed by Brizmer et al. [30, 31] using the Reynolds equation showed a significant increase in load-carrying capacity for partial texturing of parallel thrust bearings with linear motion. A ratio of texture depth to lubricant film height of 1.25 and a lateral texture length in the sliding direction of 65% were found to be favourable. This was confirmed by a tripling of the bearing clearance and a friction reduction of 50% [31]. Rahmani et al. [32] performed numerical parameter studies for the simplified case of the one-dimensional (1D) Reynolds differential equation (infinite linear sliding bearing) and non-mass-conserving cavitation model to find advantageous micro-textures. Using dimensionless parameters and analytical correlations, a genetic algorithm allowed for the optimization regarding load-carrying capacity

and friction. Rectangular textures with a maximum surface coverage and a ratio of texture depth to lubricant film height of about 0.6 proved to be favourable. Although special care should be given due to the used simplifications, the derived recommendations were in good agreement with parametric studies from Pascovici et al. [34]. Comprehensive parametric numerical studies on finite linear sliding bearings were carried out by Dobrica et al. [35]. These were based on the 2D Reynolds equation and a mass-conserving cavitation model. They showed that partial texturing, especially in the contact inlet, significantly enhances the load-carrying capacity if the oil pressure in the inflow is sufficiently high. However, this also leads to a larger lubricant film height and thus to a higher oil demand. Moreover, it was shown that the load-carrying capacity maximizes for the highest possible area coverage, which would correspond to a step bearing. These predictions were confirmed by Marian et al. [36] and Guzek et al. [37, 38]. By numerically optimizing the load-carrying capacity, the latter derived ratios of texture depth to lubricant film height between 0.7 to 0.9 as well as 1.0 to 1.2 for rectangular and elliptical textures, respectively. With the objective of friction reduction, optimal values ranged between 0.8 and 1.2. While these investigations were restricted to quasi-stationary conditions (textured stationary body), Gherca et al. [39] investigated the influence of the choice of the surfaces to be textured on the load-carrying capacity. Despite squeezing and displacement effects at the contact inlet, micro-textures on the stationary surface proved to be more effective. However, texturing both surfaces resulted in additional improvement. Based on CFD approaches by solving the Navier–Stokes equations as well as the energy equation in the fluid and heat transfer equation in the pads, Papadopoulos et al. [40–43] showed a considerable increase of the load-carrying capacity only for lower to moderate sliding velocities, while the improvement was reduced for higher velocities. However, the partially textured linear plain bearing exhibited lower friction due to the lower lubricant film height. For reciprocal sliding motion, Yu et al. [45, 46] showed that the dimensions of different texture geometries can be optimized for the respective conditions. Elliptical textures having their long semi-axis perpendicular to the sliding direction are particularly suitable. Similar conclusions were drawn by Qiu et al. [47, 48]. Shen and Khonsari [49] employed the SQP method coupled with a FDM model solving the Reynolds equation with a non-mass-conserving cavitation model to optimize the geometry of single micro-textures. The latter was described by a series of horizontal lines that evenly divided an arbitrary texture geometry in Y direction. The SQP began with an initial guess of the design variables and evaluated the objective function at the starting point. Afterward, it solved the quadratic programming sub-problems to obtain the search direction and construct a better estimate. This process was iterated until the algorithm converged to an optimal solution. Consequently, they investigated textured parallel contact cells with periodic boundaries and found different optima for uni- and bi-directional sliding in the form of chevron-shaped and trapezoidal texture elements, respectively. Fixing the area density to 30%, the authors [49] verified that the newly obtained geometries resulted in higher peak pressures and load-carrying capacity over a wide range of operating conditions compared to conventional geometries (circles, ellipses, squares, hexagons, or diamonds). Similarly, Wang et al. [68, 69] used a FDM model to solve the Reynolds equation with a mass-conserving Elrod cavitation model and applied a hybrid GA–SQP approach to optimize the texture geometry for a rotating thrust bearing. Thereby, the advantages of the GA as a global optimization algorithm with smaller local accuracy and the SQP method as a local optimization technique, which is rather sensitive to initial values, were combined (Fig. 5(a)). It was reported that small-angle chevrons (Fig. 5(b)) quite similar to those suggested in Ref. [49] for unidirectional sliding were superior compared to straight grooves and large-angle chevrons. Accordingly, lower friction was experimentally verified over a large range of rotational speeds (Fig. 5(c)).

In the series of papers, Kalliorinne et al. [338–340] adapted and applied the globally convergent method of moving asymptotes (GC–MMA) optimisation methodology to optimise the geometry of HL bearings. They used the film thickness as control variable and considered the load-carrying capacity, the coefficient of friction, and the frictional torque as the optimised

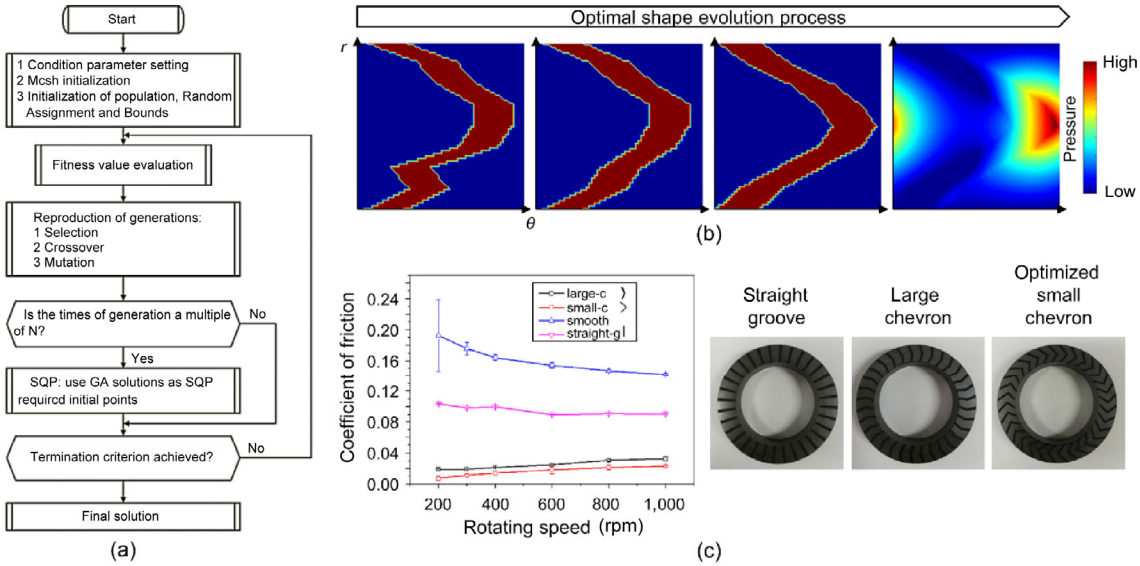

Fig. 5 (a) Flow chart of the hybrid GA–SQP method, (b) optimal shape evolution process for a texture over the radius r and the angle θ, and (c) experimentally measured coefficient of friction vs. rotating speed for smooth references as well as textured samples with straight grooves, large-angle chevron, and optimized small-angle chevron. Reproduced with permission from Ref. [68], © The Authors 2018.

targets. The methodology was verified through comparison with the Rayleigh step-bearing [341] and successors [342–350]. One important result they found, was that increasing the mesh resolution unravelled features contributes to the increased load-carrying capacity and decreased friction [339, 340]. Other results of interest are the outstanding performance and topographies of the optimised thrust bearings and washers (Fig. 6).

(3) Piston liner/ring-contacts

Based on theoretical considerations, Etsion et al. [50–54] verified a friction reduction of 30% and 45% for full and partial texturing, respectively. A significant contribution to the understanding of laser textured piston rings was made by Vlădescu et al. [55–58]. In model tests, they showed that micro-textures led to a friction increase in the centre of the stroke (full-film lubrication), but to a reduction in friction of up to 55% in the region of mixed or boundary friction during the reversal points. This was attributed to an increase in lubricant film height and reduced asperity solid contact and later substantiated by the numerical studies of Profito et al. [59, 60]. Following the numerical studies from Checo et al. [66], friction-reducing effects can also be achieved with textured cylinder liners and, above all, with piston ring surfaces that are as flat as possible with no or only slight crowning. Based on

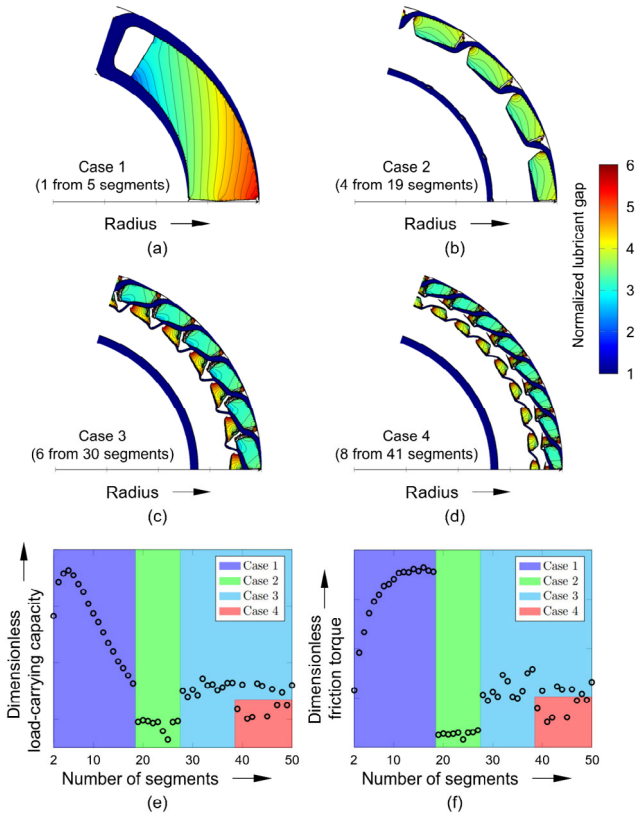

Fig. 6 (a–d) Optimal bearing geometries, (e) load-carrying capacity, and (f) frictional torque for different segmentations of the thrust pad bearing. Note that the normalized lubricant gap (the control variable) within the white areas in (a–d) saturates at the value specified as the upper limit, which in this case is 100. Reproduced with permission from Ref. [340], © IMechE 2020.

a solution of the Reynolds equation with non-mass conserving cavitation model, Zhou et al. [67] finally proposed varying texture parameters over the cylinder bore by designing the lateral dimensions of cup-shaped texture elements as a function of the respective sliding speeds. This allowed higher film thickness and load-carrying capacity than that with invariable texture parameters over the whole surface.

3.1.2 *Converging or conformal HL contacts*

(1) Tilting pad bearings

There are considerably less studies for the more complex case of non-parallel contacts. In these contacts, the macroscopic wedge shape often predominates over effects induced by micro-textures. According to Cupillard et al. [71], appropriately designed micro-textures can improve the tribological behaviour for lower convergence angles. By solving the Navier–Stokes equations using FVM without the consideration of cavitation, backflow effects for larger convergence angles and textures with a certain depth were verified, thus reducing the load-carrying capacity. Parametric study by Dobrica et al. [35] based on the 2D Reynolds equation and a mass-conserving cavitation algorithm confirmed a dependence of the load-carrying capacity and the friction reduction on the convergence angle. Furthermore, positive effects were found only for partial and not for complete texturing. In contrast, Tønder [73, 74] numerically showed better friction, damping, and stiffness properties for a fully textured tilting pad bearing. However, this was based on a non-mass-conserving cavitation model. Using 3D CFD simulations, Papadopoulos et al. [75, 76] performed an optimization of groove-shaped textures in a converging thrust bearing using a genetic algorithm, achieving an increase in load-carrying capacity of up to 7.5%. Thereby, a pressure build-up was even verified for diverging surfaces. Likewise, numerical optimization for bearings with respect to lubricant film height, friction, and temperature was performed by Gropper et al. [77] based on a FVM solution of the Reynolds equation as well as an interior-point algorithm and forward finite difference estimates. Optima were found to be independent of speed but dependent on load and optimization objective (Fig. 7). The results suggest that the gains in the bearing performance through micro-texturing are rather limited for tilting pad bearings [75–77]. In fact, tilting bearings operate under optimal conditions by design, which makes it difficult to improve their performance. This questions the usefulness of surface texturing, especially when considering increased manufacturing costs compared to untextured tilting pad bearings.

(2) Journal bearings

Initial works on radial journal bearings, for which the lubricant film height in the circumferential direction corresponds to a converging lubrication gap, go back to Tala-Ighil et al. [78, 79]. They solved the 2D Reynolds equation with a non-mass-conserving cavitation model based on the FDM. They demonstrated that micro-textures could have both a positive and a negative influence on lubricant film height, load-carrying capacity, axial flow rate, and frictional torque depending on geometry, dimensions, and arrangement. Partial texturing, especially of the area affected by pressure drop, proved to be beneficial. Ausas et al. [190] reported a small increase in the minimum lubricant film height and the frictional torque by full texturing and pointed out the relevance of mass-conserving cavitation models. Based on CFD simulations, Cupillard et al. [80] recommended smaller textures in the region of the maximum lubricant film height for low eccentricities and larger textures in the region of maximum pressure for higher eccentricities to minimize the frictional torque. However, the load carrying capacity was always worse for the textured configurations. Moreover, they showed that the influence of textures is more pronounced at lower eccentricities and beneficial texture parameters depend on the operating conditions. Similar observations were also made by Brizmer and Kligerman [81], Zhang et al. [88], and Kango et al. [82, 83]. The latter authors performed numerical simulations for different geometrical configurations of textured journal bearings, which can serve as an example of the fact that the constraints of the simulations are important when optimizing target variables not to derive invalid conclusions. Frequently, numerical work investigates the influence of micro-textures on the load-carrying capacity as derived by integrating over the pressure distribution and/or fluid friction. In case of radial journal bearings, however, the eccentricity and the attitude angle may not be assumed as fix but must be determined from the equilibrium of forces. Otherwise,

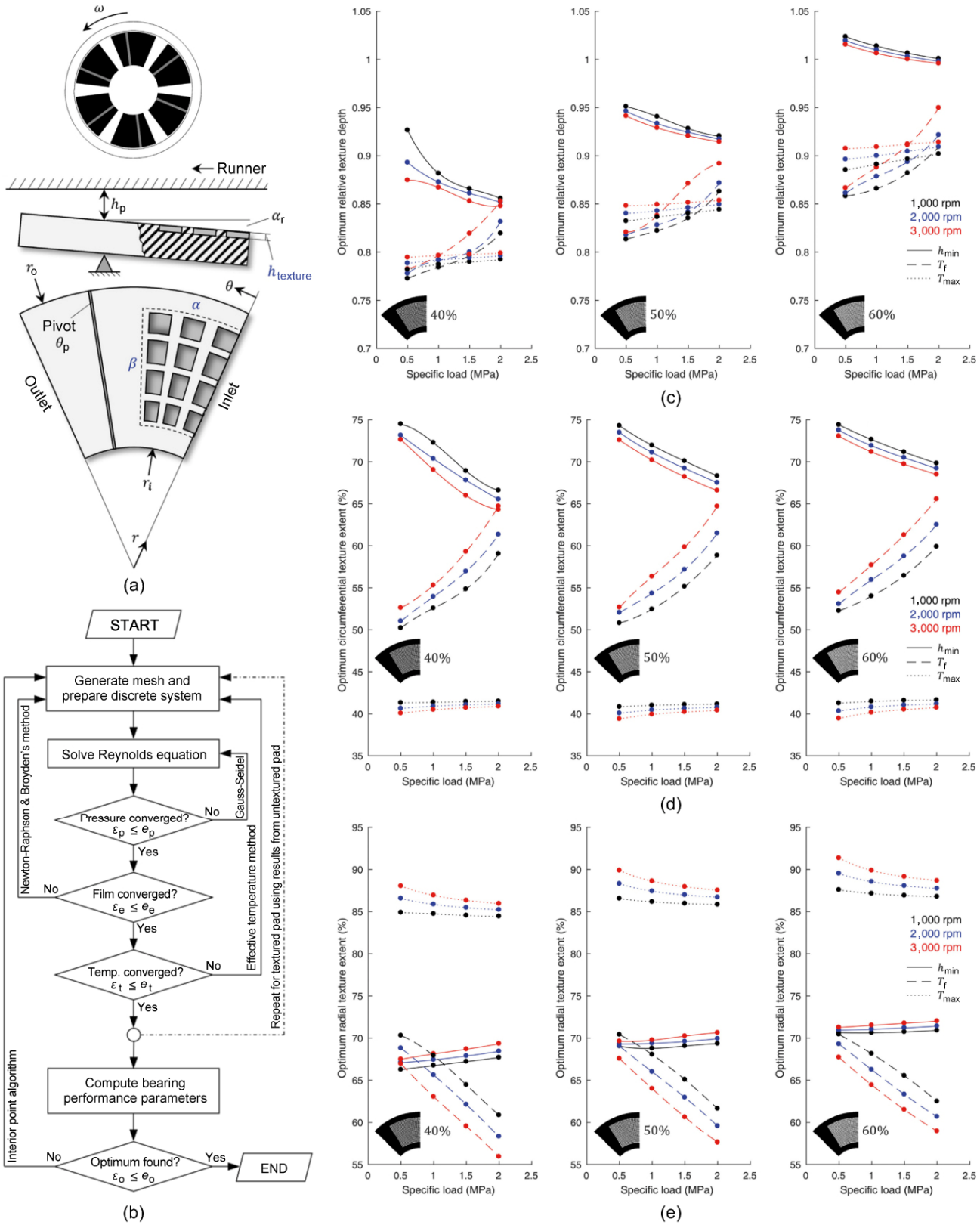

Fig. 7 (a) Micro-textured tilting pad bearing, (b) flow chart of the texture design optimization, (c) optimum relative texture depth, and (d) optimum circumferential and (e) radial texture extent at different area densities when optimizing for the minimum lubricant gap, the frictional torque, or the maximum temperature. Reproduced with permission from Ref. [77], © The Authors 2018.

it is not possible to compare the results between different textures. For instance, Cupillard et al. [80] compared friction for the same constant load. Yamada et al. [86, 87] demonstrated that the load-carrying capacity decreased for a fully textured bushing, i.e. the minimum film thickness was lowered compared to the reference state (untextured bushing). However, they demonstrated that, for given operating conditions, the higher resulting eccentricity and smaller attitude angle allowed to improve the dynamic properties of textured journal bearings. These findings confirm that the load-carrying capacity is downgraded for fully textured bushings, thus agreeing well with Refs. [78, 79] since improvements of partially textured journal bearing are obtained for specific operating conditions (low eccentricity, i.e. lower-loaded bearings) or specific textured configurations (textured zone at the beginning of the cavitation region).

3.2 EHL contacts

The effects of micro-textures on the tribological behaviour of EHL contacts have been much less studied and are not yet fully understood [10]. This can be traced back to the comparatively small, lubricated conjunction between the elastically deformed contact surfaces. Too large texture elements due to manufacturing limitations allow the lubricant to flow out of the contact area [90, 104]. Furthermore, the forming lubricant gap is several times smaller than that in sliding contacts without elastic deformation, which implies that the effects of the surface topography or even single micro-texture elements are more pronounced. The formation of a load-carrying fluid film in EHL contacts is due to the pressure-induced increase in viscosity, which can be reduced by deep textures [100]. It is often considered that the surfaces of rolling contacts subjected to higher loads should be as smooth as possible to avoid fatigue damage. However, some studies proved that micro-textures can also improve the tribological behaviour of EHL rolling–sliding contacts. Various experimental investigations based on optical interferometry and artificially created regular surface topographies as well as numerical work indicated that grooves or ribs arranged perpendicular to the direction of motion can increase the lubricant film height in EHL point contacts. Parallel elements showed rather negative effects on the lubricant film formation [351, 352].

3.2.1 *Hard EHL contacts*

Initial experimental studies on discrete micro-textures in hard EHL point contacts were realized by Cusano and Wedeven [95, 96]. It was demonstrated that the lubricant gap was reduced in the area around the depressions, which was more pronounced at the leading edge and for elongated textures in rolling direction. With increasing slip, however, there was an additional, local widening in the fluid film height in front of or behind the texture, depending on whether the untextured or textured body was moving faster. Similarly, Dumont et al. [110] numerically demonstrated for a point contact under full and starved lubrication that the volume of the texture elements was reduced by elastic deformation during the traversal of the contact area, thus releasing additional fluid and increasing the lubricant gap. Using optical interferometry and numerical EHL modelling with an MG solver, Mourier et al. [99, 100] verified that deeper textures reduced the fluid film height, while shallow ones tended to increase the lubricant gap. This was attributed to the highly viscous lubricant, which was drawn out of the micro-depression due to shear effects, leading to additional local elastic deformation. Furthermore, it was shown that the compressed lubricant was not dragged out until the entire texture was within the contact area. This suggested that optimal texture parameters do exist for widening the lubricant gap. It is important to mention that less beneficial or even detrimental effects occur when exceeding or surpassing these values. Křupka et al. [101–103, 105, 109] confirmed the decisive role of the fluid viscosity and velocity differences of the contacting bodies (slip) as well as flat textures. Well-designed micro-textures in very thin film EHL contacts reduced the interactions of surface roughness/solid asperities and friction. The basic mechanisms are exemplified in Fig. 8 for the passage of a single micro-texture through a point contact under pure sliding and mixed lubrication conditions (load parameter $M = 185$, viscosity parameter $L = 13$, slide-to-roll-ratio $SRR = -2$). The results shown were obtained from a transient thermo-elastohydrodynamic lubrication (TEHL) simulation

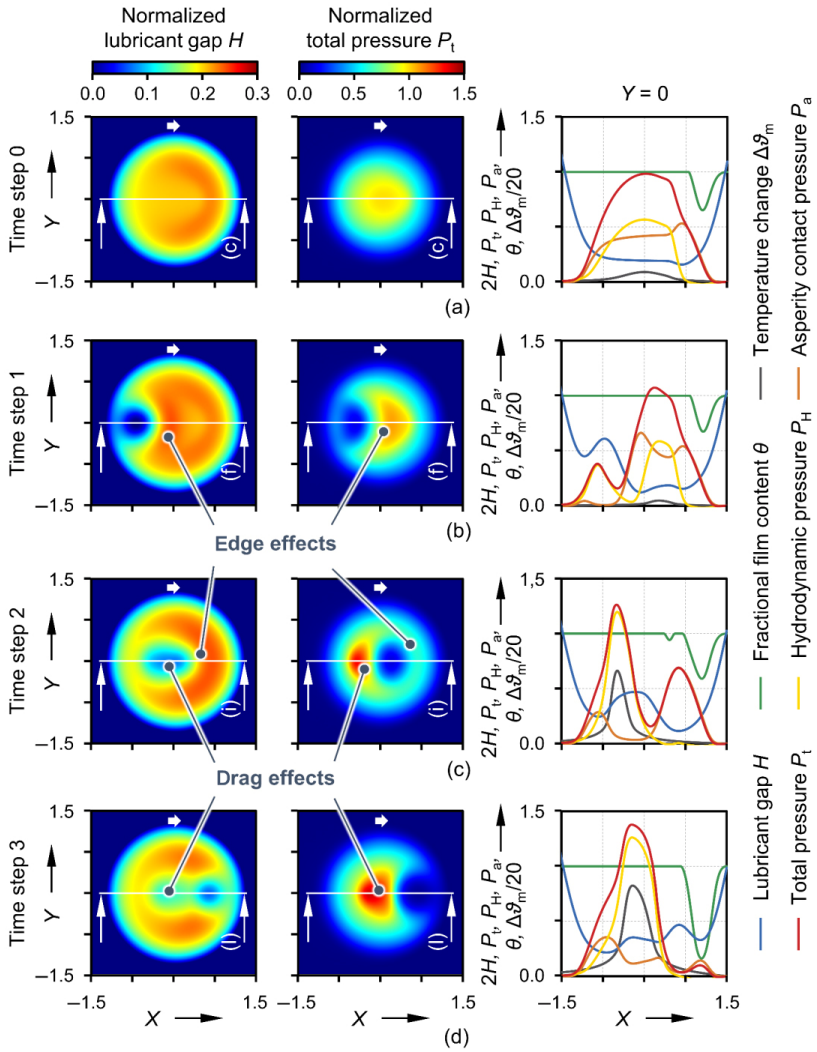

Fig. 8 Lubricant gap and total pressure distribution over the normalized contact length (X) and width (Y) as well as fluid film height, fractional film content, temperature, total, hydrodynamic, and asperity contact pressure in the $Y = 0$ cross-section: (a) without micro-texture, (b) with a single micro-texturing when entering, and (c) in the middle as well as (d) when leaving the contact area. Reproduced with permission from Ref. [140], © The Authors 2021.

model based upon the FEM full system approach with a stochastic mixed friction and a mass-conserving cavitation model [133, 136, 140].

Wang et al. [125] carried out ball-on-disk experiments and numerical investigations based upon the Reynolds equation with a mass-conserving cavitation model including mixed friction, thus correlating the lubricant film enlargement with the friction reduction. Elongated textures oriented transversely to the motion with a triangular cross-section were deduced to be beneficial. Marian et al. [133, 140] employed a meta-model of optimal prognosis (MOP) [353, 354] to study the influence of depth and diameter of a single cup-shaped micro-texture. Non-significant variables were first filtered before various meta-models, such as polynomial regression, MLS, and kriging, were trained. The most suitable approach was then automatically selected using a coefficient of prognosis, and the response surfaces (Fig. 9) were used for optimization by an EA with the goal of minimizing solid state friction. With boundary conditions against excessive wear/fatigue (limiting the minimum lubricant film height and maximum pressure), flat textures with depths of a few microns and lateral dimensions close to the elastically deformed contact area were identified as optimal and robust. Although only a single texture was optimized, the authors point out that the methods can also be used to effectively tailor textures [133].

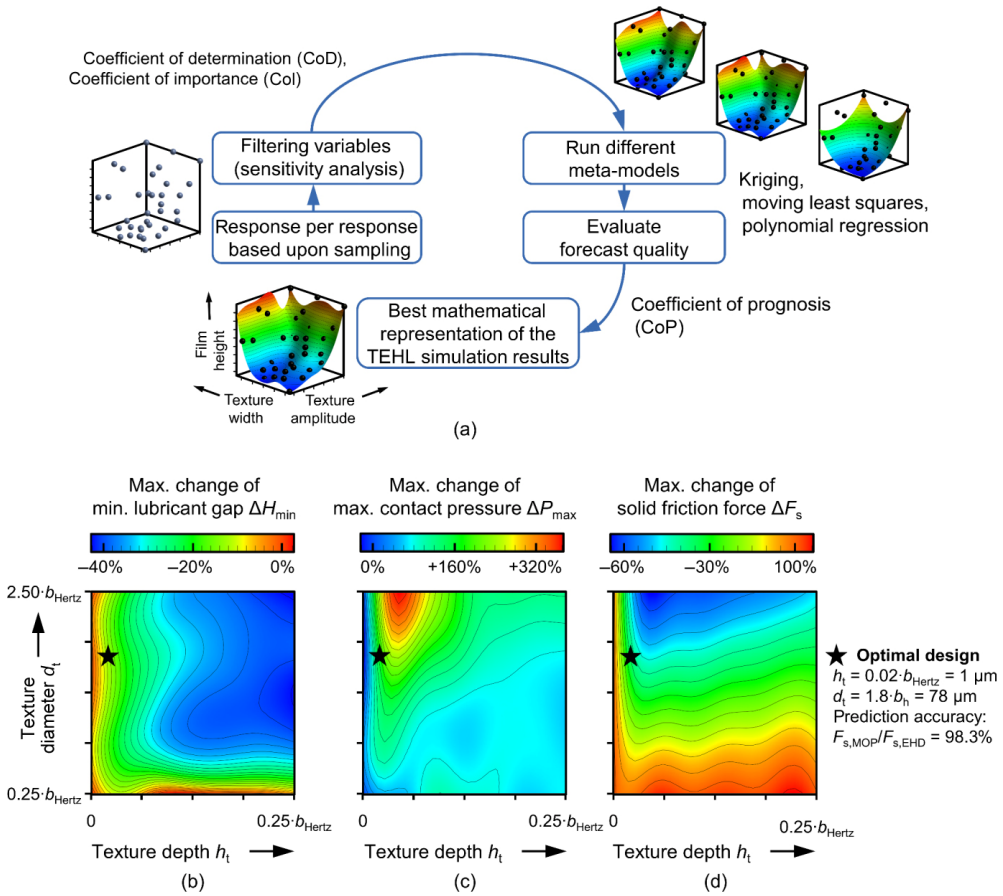

Fig. 9 (a) Framework and response surfaces of a MOP for the maximum changes of (b) minimum lubricant gap, (c) maximum contact pressure, and (d) solid friction force dependent on micro-texture depth and diameter. The result of a multi-objective optimization by an EA is indicated by a star. Reproduced with permission from Ref. [133], © Elsevier Ltd. 2019; Ref. [140], © The Authors 2021; Ref. [318], © The Authors 2020.

Besides EHL simulation, numerical optimization has been carried out using experimental data. De La Guerra Ochoa et al. [138] used friction results from a mini traction machine (ball-on-disk) with different cup-shape textures under various operating conditions to train an ANN. Generally, textures were able to reduce friction especially at low sliding speeds and a small texture radius with a rather high area density was reported to be most beneficial. Boidi et al. [139, 355] employed a Hardy multiquadric radial base function to predict the wear behaviour of sintered components under varying operating conditions in a ball-on-disk setup (mini-traction machine and lubricant film thickness measurements based on optical interferometry) as well as geometric or statistical characteristics of the dimples, grooves, and pores.

Furthermore, model-level investigations have been performed on micro-textures in line or elliptical EHL contacts. Numerical work from Zhai et al. [120] considering surface roughness indicates that micro-dents in highly-loaded line contacts under almost pure rolling did not induce an improved fatigue life. In numerical studies on the start-up behaviour of line contacts and stationary textures, Zhao and Sadeghi [122] showed the earlier build-up of a separating lubricating film. In experiments with crowned, textured disc surfaces and numerical studies based on the Reynolds equation and elastic half-space, Pausch [124] showed a widening of the lubricant behind the texture as well as a reduction at the rear and lateral edges, which could fall below the constriction of the smooth contact. This was more pronounced for discontinuous cross sections and deep textures than for continuous and shallow ones.

Due to the scarcely improved or even degraded fluid film formation by micro-textures in EHL contacts,

there are only a few successful, application-oriented investigations on highly-loaded machine elements under rolling conditions, e.g. rolling bearings. Particularly for the latter, the surface roughness or topography has a decisive influence on rolling fatigue [356] as a result of cyclically induced pressure and stress peaks [357, 358]. However, Vrbka et al. [359] suggested that depressions may act as fluid reservoirs, especially at smaller film heights, which allowed the lubricant to be supplied to the contact after all. An increase in fatigue life was attributed to reduced material shear stress due to lower friction [11]. According to numerical investigations on radial ball bearings by Shi et al. [127], even small slip states tend to increase the formed lubricant film height by hydrodynamic effects, thus enhancing the fatigue life.

For tooth flank contacts of gears, there is also a general trend toward superfinished [360] or coated [361, 362] surfaces to increase energy efficiency and prevent component failure by pitting or fretting. Generally, the contact is characterized by higher loads, low lubricant film heights, and varying sliding/rolling conditions along the line of contact [130]. Because of these harsh conditions, only a few works have dealt with the texturing of tooth flanks, indicating that the tribological behaviour can rather be improved for low speed and mixed friction only [123].

The cam/tappet contact of the valve train is another tribological system subject to high loads and sliding portions. Frequently, the surfaces are mirror-polished and/or coated [363–365]. However, Gangopadhyay and McWatt [129] determined up to 35% lower friction in tests on a dragged cylinder head for V-shaped textures compared to isotropically polished cup tappets. Kang et al. [132] demonstrated 34% reduced stroke losses and reduced wear after 300 h of operation for a cam with textured flanks in contact with the roller cam follower of a single-cylinder diesel engine. Recently, Marian et al. [134] showed a friction reduction of up to 13% on a component test-rig operating under mixed lubrication by introducing line-shaped textures with an orientation perpendicular to the sliding direction on bucket tappet surfaces. Furthermore, long-term tests revealed that deeper micro-textures with smaller lateral distances featured higher wear, which was ascribed to the intensified edge effects around the textures and an additional necking in the lubricant film height. Marian et al. [137, 140] employed a MOP and an EA to optimize the micro-texture dimensions. Flat textures with lateral dimensions close to the elastically deformed contact were found to be most beneficial for reducing asperity contact and solid friction. The distance of the textures in sliding directions had to be designed in such a way that trailing texture elements did not influence the drag effects of the leading ones. Moreover, no friction-reducing effects were determined for higher rotational speeds (only slight mixed or even full-film lubrication). The trailing effects induced by the micro-textures, which lead to the local fluid film enlargement, were accompanied by an increase in lubricant viscosity due to the build-up of additional hydrodynamic pressure and thus an increase in the fluid traction [135].

3.2.2 *Soft EHL contacts*

Some studies have focused on micro-textures in lower-loaded contacts with at least one soft material and thus elastic deformation. The elastic deformation and surface topography have also a substantial influence on the resulting tribological behaviour [366, 367]. Hadinata and Stephens [141] developed a Reynolds-based simulation model for the contact of textured shaft with a smooth elastomer rotary seal, and thus demonstrated an increased load-carrying capacity and reduced friction. For similar conditions, Shinkarenko et al. [142–144] numerically verified the validity of the assumption of linear elastic material behaviour, thus deriving the optimal texture parameters. Depending on the material properties, area coverages between 30% and 50% as well as aspect ratios between 0.05 and 0.1 proved to be advantageous. Moreover, texturing the elastomer seal instead of the shaft was suggested due to the smaller surface area. Warren and Stephen [145] and Li et al. [146] compared experimental investigations with numerical results based on the Reynolds equation with mass-conserving cavitation model and under consideration of nonlinear material behaviour. In good qualitative agreement, it could be shown that micro-elevations increased the load-bearing capacity more than depressions.

Furthermore, various studies on micro-textures have been carried out in the field of biomaterials and medical technology, e.g. load-bearing artificial implants [15, 368–370]. For instance, Dougherty et al. [151]

numerically modelled the contact between a micro-textured ultra-high molecular weight polyethylene (UHMWPE) disc with a steel pin under water lubrication and reported a shift in the Stribeck curve as well as a friction reduction of up to 50%. Chyr et al. [148] studied a conformal pairing of UHMWPE shell and textured cobalt–chromium (CoCr) alloy cylinder under pivoting motion and used a rather simple numerical model that solved the Reynolds equation while neglecting elastic deformations to trace friction reduction back to an increase in the load-carrying capacity. Gao et al. [150] established a simulation model of artificial knee implants based on the Reynolds equation and the MG method as well as FFT into spherical coordinates, which was coupled with an adapted Archard wear formula. Although the underlying mechanism was not addressed, it was reported that cup-shaped textures improved the lubrication conditions and wear behaviour in lateral contact, while no beneficial effects were found on the medial side. Recently, Marian et al. [140, 371, 372] used a full-system FEM-based model considering mass-conserving cavitation and mixed lubrication to study the influence of micro-textures on the performance of total knee replacements. Despite velocity differences of the contacting partners and textures experiencing considerable elastic deformation, only rather minor edge and the drag effects appeared in comparison with the hard EHL contacts considered in the previous section. For the systematic analysis of the influence as well as for the optimization of depth, diameter, and separation of the texture elements, a MOP was generated from a LHS database. While small texture distances and deep textures led to an increased solid friction, pronounced minima were found for rather flat textures with either a very small or large diameter. It was concluded that an optimization of the macro-geometry, e.g. the conformity of femoral and tibial components, may have a higher influence on the lubrication conditions and the wear of the femur than modifying the micro-topography.

4 Challenges, opportunities, and concluding remarks

Nature provides numerous examples of surface topographies tailored for specific conditions. Inspired by that, micro-textures applied to rubbing surfaces in hydro- or elastohydrodynamically lubricated contacts can reduce energy losses by reducing friction and/or wear. Although this approach has already received considerable attention over decades, quantitative conclusions are not readily available, and surface texturing is still in the trial-and-error-phase. To reduce this trial-and-error approach, there is an urgent need for further numerical optimization to predict the best texture parameters and arrangements for specific applications. In this regard, comparatively few works successfully applied numerical optimization strategies going beyond simple parametric studies. Existing state-of-the-art studies are summarized in Table 5 and serve as frameworks to tailor micro-textures dependent on the respective contact type and the operating conditions, which may promote their industrial scale implementation in various applications.

Based upon our analysis, the main findings can be summarized as follows:

1) For parallel HL contacts, such as mechanical seals, thrust bearings, or piston-liner contacts, full surface texturing leads to a slight improvement in the load-bearing capacity and the frictional behaviour. More significant effects can be achieved by partially texturing the contact inlet or reversal points of motion. In case of rotating parallel contacts, optimal texture parameters can be found, especially aspect

Table 5 Numerical optimization approaches to tailor micro-textures.

Lubrication regime and application	Optimization approach	Ref.
Parallel HL contacts	NSGA (direct)	[70]
	Adjoint optimization technique (direct)	[89]
	GA (direct)	[32, 33]
	SQP (direct)	[49]
	GA–SQP (direct)	[68, 69]
	GC–MMA (direct)	[338–340]
Converging HL contacts	GA (direct)	[75, 76]
	Interior-point algorithm (direct)	[77]
	PSO (direct)	[88]
EHL contacts	MOP + GA (indirect)	[133, 137]
	ANN (indirect)	[138]

ratio and area coverage ratio. However, in contrast to linear sliding parallel contacts, the optima strongly depend on the operating conditions. For application-related conditions, the design of micro-textures for specific load cases or situations usually represents a compromise regarding the entire stress spectrum. To fully exploit the energy-saving effects of surface micro-textures, they need to be optimized locally for the respective regions of the components' surfaces. Moreover, the geometries of the micro-textures can be described more flexibly to optimize different cross-sectional geometries or even surface topographies at different scales. This may allow even more substantial friction-reductions and energy-savings than achieved by deterministic, single-scale textures. Direct optimization methods such as GA or SQP are of special interest. By combining both approaches, synergistic effects between global and local optimization algorithms can be achieved, thus leading to more accurate predictions. Furthermore, topology optimization methods offer design options with a very high degree of geometric freedom. In the future, methods for turning the obtained optima to dimensionable and manufacturable geometries could become relevant.

2) For converging or conformal HL contacts (tilting pad or radial journal bearings), the influence of micro-textures and favourable geometric parameters of the textures depends on the operating conditions. For lower-loaded applications, notable improvements for load-carrying capacity and friction can be achieved. In contrast, the load-carrying capacity improvement is either very limited or impossible while an improvement in friction and/or dynamic performance can be obtained for severe conditions with pronounced convergence ratios of thrust bearings and sliders or high eccentricities for journal bearings. For these configurations, achievable improvements are generally smaller than for (almost) parallel surfaces, while partial texturing is often preferable. Unfavourably designed textures result in downgraded frictional properties. Therefore, numerical optimization is of essential importance. Occasionally, studies with contradicting results regarding the boundary conditions of the tribo-simulation and the target variables of the optimization (comparison of friction at different load cases) can be found in literature. Therefore, we emphasize that the boundary conditions of the simulations, on which the optimization is based, must be appropriately selected to generate meaningful predictions. The aforementioned methods of direct optimization can also be employed, e.g. GA, SQP, or topology optimization.

3) For EHL contacts, such as rolling bearings, gears, and cam-followers, well-designed micro-textures can reduce friction and/or wear, which holds especially true for a sufficient amount of slip and mixed lubrication due to reduced solid asperity contact. The application of surface textures in pure rolling of high load conditions has rather negative effects. Flat textures oriented transversely to the direction of motion with lateral dimensions smaller than the elastically deformed contact area proved to be beneficial. The spacing between textures needs to be optimized that edge effects originating from the trailing texture elements do not negatively affect the drag effects of the leading ones. Due to the higher computational costs and the necessity to consider time-transient effects, indirect approaches with intermediate surrogate or meta-models that were trained within DoEs are particularly suitable for optimizing micro-textures in EHL contacts. In the future, these methods can also be extended to design multiscale textures by a freer parameterization and to adapt them locally on the surfaces of gear tooth flanks, tappets, or implants. Thus, areas that generally experience full film lubrication can be left untextured, and only regions with mixed friction conditions and sufficiently high sliding portions can be provided with optimal textures.

4) Most of the numerical modelling and optimization approaches that can be found in literature focus on improving the energy efficiency in terms of maximizing the load-carrying capacity to prevent wear or minimizing frictional losses. This implies that numerical modelling of the involved wear processes in micro-textured contacts under mixed lubrication is considered as a highly promising and challenging future research direction.

5) Most of the applications with HL and EHL contacts do not operate under steady state conditions, and the optimization of surface micro-textures always represents a certain trade-off or compromise. By means

of optimization algorithms, micro-textures should be designed in a robust way to be resilient against inaccurate load or kinematic assumptions, manufacturing deviations of the micro-texture geometries or component misalignment. In this context, multi-scale textures can potentially be designed in such a way that positive effects are achieved for a variety of loads or even under more extreme conditions. In the future, ML/AI approaches will gain in importance, especially due to the complexity of the optimization tasks and the associated computational effort.

6) Surface micro-textures represent an important trend to tailor friction and/or wear. In the future, synergistic effects with lubricant rheology and other surface modification approach, such as the application of thin coatings, will come more into focus.

Appendix Prisma flowchart of the systematic literature review

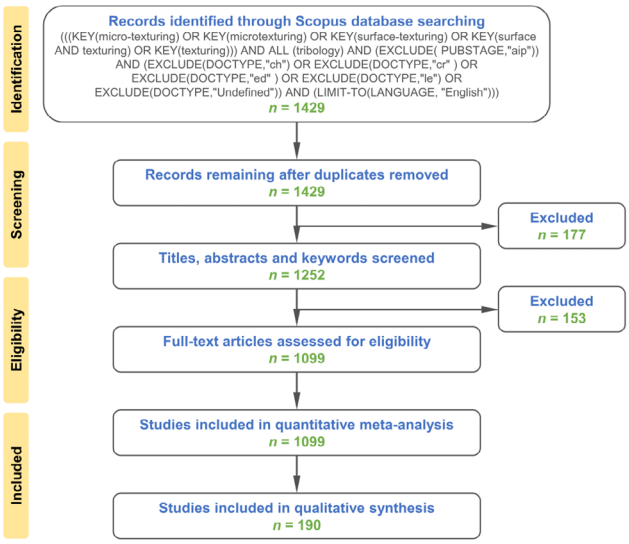

Acknowledgements

Max MARIAN greatly acknowledges the support from Pontificia Universidad Católica de Chile. Andreas ALMQVIST acknowledges the financial support from The Swedish Research Council (VR): DNR 2019-04293. Andreas ROSENKRANZ gratefully acknowledges the financial support given by ANID within the project Fondequip EQM190057 as well as the University of Chile in the project U-Moderniza UM-04/19.

Declaration of competing interest

The authors declare no conflict of interest.

References

[1] Hamilton D B, Walowit J A, Allen C M. A theory of lubrication by microirregularities. *J Basic Eng* **88**(1): 177–185 (1966)

[2] Anno J N, Walowit J A, Allen C M. Load support and leakage from microasperity-lubricated face seals. *J Lubr Technol* **91**(4): 726–731 (1969)

[3] Anno J N, Walowit J A, Allen C M. Microasperity lubrication. *J Lubr Technol* **90**(2): 351–355 (1968)

[4] Henry Y, Bouyer J, Fillon M. Experimental analysis of the hydrodynamic effect during start-up of fixed geometry thrust bearings. *Tribol Int* **120**: 299–308 (2018)

[5] Dadouche A, Conlon M J. Operational performance of textured journal bearings lubricated with a contaminated fluid. *Tribol Int* **93**: 377–389 (2016)

[6] Gropper D, Wang L, Harvey T J. Hydrodynamic lubrication of textured surfaces: A review of modeling techniques and key findings. *Tribol Int* **94**: 509–529 (2016)

[7] Sudeep U, Tandon N, Pandey R K. Performance of lubricated rolling/sliding concentrated contacts with surface textures: A review. *J Tribol* **137**(3): 031501 (2015)

[8] Dobrica M B, Fillon M. About the validity of Reynolds equation and inertia effects in textured sliders of infinite width. *Proc Inst Mech Eng Part J J Eng Tribol* **223**(1): 69–78 (2009)

[9] Arghir M, Roucou N, Helene M, Frene J. Theoretical analysis of the incompressible laminar flow in a macro-roughness cell. *J Tribol* **125**(2): 309–318 (2003)

[10] Gachot C, Rosenkranz A, Hsu S M, Costa H L. A critical assessment of surface texturing for friction and wear improvement. *Wear* **372–373**: 21–41 (2017)

[11] Rosenkranz A, Grützmacher P G, Gachot C, Costa H L. Surface texturing in machine elements—A critical discussion for rolling and sliding contacts. *Adv Eng Mater* **21**(8): 1900194 (2019)

[12] Grützmacher P G, Profito F J, Rosenkranz A. Multi-scale surface texturing in tribology—Current knowledge and future perspectives. *Lubricants* **7**(11): 95 (2019)

[13] Lu P, Wood R J K. Tribological performance of surface texturing in mechanical applications—A review. *Surf Topogr*: *Metrol Prop* **8**(4): 043001 (2020)

[14] Rosenkranz A, Costa H L, Baykara M Z, Martini A. Synergetic effects of surface texturing and solid lubricants to tailor friction and wear—A review. *Tribol Int* **155**: 106792 (2021)

[15] Allen Q, Raeymaekers B. Surface texturing of prosthetic hip implant bearing surfaces: A review. *J Tribol* **143**(4): 040801 (2021)

[16] Etsion I, Burstein L. A model for mechanical seals with regular microsurface structure. *Tribol Trans* **39**(3): 677–683 (1996)

[17] Etsion I, Kligerman Y, Halperin G. Analytical and experimental investigation of laser-textured mechanical seal faces. *Tribol Trans* **42**(3): 511–516 (1999)

[18] Etsion I, Halperin G. A laser surface textured hydrostatic mechanical seal. *Tribol Trans* **45**(3): 430–434 (2002)

[19] Etsion I. Improving tribological performance of mechanical components by laser surface texturing. *Tribol Lett* **17**(4): 733–737 (2004)

[20] Bai S X, Peng X D, Li Y F, Sheng S E. A hydrodynamic laser surface-textured gas mechanical face seal. *Tribol Lett* **38**(2): 187–194 (2010)

[21] Meng X K, Bai S X, Peng X D. Lubrication film flow control by oriented dimples for liquid lubricated mechanical seals. *Tribol Int* **77**: 132–141 (2014)

[22] Brunetière N, Tournerie B. Numerical analysis of a surface-textured mechanical seal operating in mixed lubrication regime. *Tribol Int* **49**: 80–89 (2012)

[23] Qiu Y, Khonsari M M. On the prediction of cavitation in dimples using a mass-conservative algorithm. *J Tribol* **131**(4): 041702 (2009)

[24] Qiu Y, Khonsari M M. Performance analysis of full-film textured surfaces with consideration of roughness effects. *J Tribol* **133**(2): 021704 (2011)

[25] Qiu Y, Khonsari M M. Experimental investigation of tribological performance of laser textured stainless steel rings. *Tribol Int* **44**(5): 635–644 (2011)

[26] Wang X L, Kato K, Adachi K, Aizawa K. Loads carrying capacity map for the surface texture design of SiC thrust bearing sliding in water. *Tribol Int* **36**(3): 189–197 (2003)

[27] Wang X L, Adachi K, Otsuka K, Kato K. Optimization of the surface texture for silicon carbide sliding in water. *Appl Surf Sci* **253**(3): 1282–1286 (2006)

[28] Zhang H, Zhang D Y, Hua M, Dong G N, Chin K S. A study on the tribological behavior of surface texturing on Babbitt alloy under mixed or starved lubrication. *Tribol Lett* **56**(2): 305–315 (2014)

[29] Zhang J G, Zhang J J, Rosenkranz A, Suzuki N, Shamoto E. Frictional properties of surface textures fabricated on hardened steel by elliptical vibration diamond cutting. *Precis Eng* **59**: 66–72 (2019)

[30] Brizmer V, Kligerman Y, Etsion I. A laser surface textured parallel thrust bearing. *Tribol Trans* **46**(3): 397–403 (2003)

[31] Etsion I, Halperin G, Brizmer V, Kligerman Y. Experimental investigation of laser surface textured parallel thrust bearings. *Tribol Lett* **17**(2): 295–300 (2004)

[32] Rahmani R, Shirvani A, Shirvani H. Optimization of partially textured parallel thrust bearings with square-shaped micro-dimples. *Tribol Trans* **50**(3): 401–406 (2007)

[33] Rahmani R, Mirzaee I, Shirvani A, Shirvani H. An analytical approach for analysis and optimisation of slider bearings with infinite width parallel textures. *Tribol Int* **43**(8): 1551–1565 (2010)

[34] Pascovici M D, Cicone T, Fillon M, Dobrica M B. Analytical investigation of a partially textured parallel slider. *Proc Inst Mech Eng Part J J Eng Tribol* **223**(2): 151–158 (2009)

[35] Dobrica M B, Fillon M, Pascovici M D, Cicone T. Optimizing surface texture for hydrodynamic lubricated contacts using a mass-conserving numerical approach. *Proc Inst Mech Eng Part J J Eng Tribol* **224**(8): 737–750 (2010)

[36] Marian V G, Kilian M, Scholz W. Theoretical and experimental analysis of a partially textured thrust bearing with square dimples. *Proc Inst Mech Eng Part J J Eng Tribol* **221**(7): 771–778 (2007)

[37] Guzek A, Podsiadlo P, Stachowiak G W. A unified computational approach to the optimization of surface textures: One dimensional hydrodynamic bearings. *Tribol Online* **5**(3): 150–160 (2010)

[38] Guzek A, Podsiadlo P, Stachowiak G W. Optimization of textured surface in 2D parallel bearings governed by the Reynolds equation including cavitation and temperature. *Tribol Online* **8**(1): 7–21 (2013)

[39] Gherca A, Fatu A, Hajjam M, Maspeyrot P. Effects of surface texturing in steady-state and transient flow conditions: Two-dimensional numerical simulation using a mass-conserving cavitation model. *Proc Inst Mech Eng Part J J Eng Tribol* **229**(4): 505–522 (2015)

[40] Charitopoulos A, Fouflias D, Papadopoulos C I, Kaiktsis L, Fillon M. Thermohydrodynamic analysis of a textured sector-pad thrust bearing: Effects on mechanical deformations. *Mech Ind* **15**(5): 403–411 (2014)

[41] Papadopoulos C I, Kaiktsis L, Fillon M. Computational fluid dynamics thermohydrodynamic analysis of three-dimensional sector-pad thrust bearings with rectangular dimples. *J Tribol* **136**(1): 011702 (2014)

[42] Papadopoulos C I, Efstathiou E E, Nikolakopoulos P G, Kaiktsis L. Geometry optimization of textured three-dimensional micro- thrust bearings. *J Tribol* **133**(4): 041702 (2011)

[43] Fouflias D G, Charitopoulos A G, Papadopoulos C I, Kaiktsis L, Fillon M. Performance comparison between textured, pocket, and tapered-land sector-pad thrust bearings using computational fluid dynamics thermohydrodynamic analysis. *Proc Inst Mech Eng Part J J Eng Tribol* **229**(4): 376–397 (2015)

[44] Henry Y, Bouyer J, Fillon M. An experimental analysis of the hydrodynamic contribution of textured thrust bearings during steady-state operation: A comparison with the untextured parallel surface configuration. *Proc Inst Mech Eng Part J J Eng Tribol* **229**(4): 362–375 (2015)

[45] Yu H, Deng H, Huang W, Wang X L. The effect of dimple shapes on friction of parallel surfaces. *Proc Inst Mech Eng Part J J Eng Tribol* **225**(8): 693–703 (2011)

[46] Yu H W, Wang X L, Zhou F. Geometric shape effects of surface texture on the generation of hydrodynamic pressure between conformal contacting surfaces. *Tribol Lett* **37**(2): 123–130 (2010)

[47] Qiu M F, Delic A, Raeymaekers B. The effect of texture shape on the load-carrying capacity of gas-lubricated parallel slider bearings. *Tribol Lett* **48**(3): 315–327 (2012)

[48] Qiu M F, Minson B R, Raeymaekers B. The effect of texture shape on the friction coefficient and stiffness of gas-lubricated parallel slider bearings. *Tribol Int* **67**: 278–288 (2013)

[49] Shen C, Khonsari M M. Numerical optimization of texture shape for parallel surfaces under unidirectional and bidirectional sliding. *Tribol Int* **82**: 1–11 (2015)

[50] Ryk G, Etsion I. Testing piston rings with partial laser surface texturing for friction reduction. *Wear* **261**(7–8): 792–796 (2006)

[51] Ryk G, Kligerman Y, Etsion I, Shinkarenko A. Experimental investigation of partial laser surface texturing for piston-ring friction reduction. *Tribol Trans* **48**(4): 583–588 (2005)

[52] Ryk G, Kligerman Y, Etsion I. Experimental investigation of laser surface texturing for reciprocating automotive components. *Tribol Trans* **45**(4): 444–449 (2002)

[53] Ronen A, Etsion I, Kligerman Y. Friction-reducing surface-texturing in reciprocating automotive components. *Tribol Trans* **44**(3): 359–366 (2001)

[54] Etsion I, Sher E. Improving fuel efficiency with laser surface textured piston rings. *Tribol Int* **42**(4): 542–547 (2009)

[55] Vlădescu S C, Olver A V, Pegg I G, Reddyhoff T. The effects of surface texture in reciprocating contacts—An experimental study. *Tribol Int* **82**: 28–42 (2015)

[56] Vlădescu S C, Olver A V, Pegg I G, Reddyhoff T. Combined friction and wear reduction in a reciprocating contact through laser surface texturing. *Wear* **358–359**: 51–61 (2016)

[57] Vlădescu S C, Ciniero A, Tufail K, Gangopadhyay A, Reddyhoff T. Looking into a laser textured piston ring–liner contact. *Tribol Int* **115**: 140–153 (2017)

[58] Vlădescu S C, Medina S, Olver A V, Pegg I G, Reddyhoff T. Lubricant film thickness and friction force measurements in a laser surface textured reciprocating line contact simulating the piston ring–liner pairing. *Tribol Int* **98**: 317–329 (2016)

[59] Profito F J, Vladescu S C, Reddyhoff T, Dini D. Experimental validation of a mixed-lubrication regime model for textured piston–ring–liner contacts. *Matls Perf Charact* **6**(2): MPC20160019 (2017)

[60] Profito F J, Vlădescu S C, Reddyhoff T, Dini D. Transient experimental and modelling studies of laser-textured micro-grooved surfaces with a focus on piston–ring cylinder liner contacts. *Tribol Int* **113**: 125–136 (2017)

[61] Morris N, Rahmani R, Rahnejat H, King P D, Fitzsimons B. Tribology of piston compression ring conjunction under transient thermal mixed regime of lubrication. *Tribol Int* **59**: 248–258 (2013)

[62] Shen C, Khonsari M M. The effect of laser machined pockets on the lubrication of piston ring prototypes. *Tribol Int* **101**: 273–283 (2016)

[63] Shen C, Khonsari M M. Tribological and sealing performance of laser pocketed piston rings in a diesel engine. *Tribol Lett* **64**(2): 26 (2016)

[64] Morris N, Rahmani R, Rahnejat H, King P D, Howell-Smith S. A numerical model to study the role of surface textures at top dead center reversal in the piston ring to cylinder liner contact. *J Tribol* **138**(2): 021703 (2016)

[65] Morris N, Leighton M, de La Cruz M, Rahmani R, Rahnejat H, Howell-Smith S. Combined numerical and experimental investigation of the micro-hydrodynamics of chevron-based textured patterns influencing conjunctional friction of sliding contacts. *Proc Inst Mech Eng Part J J Eng Tribol* **229**(4): 316–335 (2015)

[66] Checo H M, Ausas R F, Jai M, Cadalen J P, Choukroun F, Buscaglia G C. Moving textures: Simulation of a ring sliding on a textured liner. *Tribol Int* **72**: 131–142 (2014)

[67] Zhou Y K, Zhu H, Tang W, Ma C B, Zhang W Q. Development of the theoretical model for the optimal design of surface texturing on cylinder liner. *Tribol Int* **52**: 1–6 (2012)

[68] Wang W, He Y Y, Zhao J, Mao J Y, Hu Y T, Luo J B. Optimization of groove texture profile to improve hydrodynamic lubrication performance: Theory and experiments. *Friction* **8**(1): 83–94 (2020)

[69] Wang W, He Y Y, Zhao J, Li Y, Luo J B. Numerical optimization of the groove texture bottom profile for thrust bearings. *Tribol Int* **109**: 69–77 (2017)

[70] Wang X Y, Shi L P, Dai Q W, Huang W, Wang X L. Multi-objective optimization on dimple shapes for gas face seals. *Tribol Int* **123**: 216–223 (2018)

[71] Cupillard S, Cervantes M J, Glavatskih S. Pressure buildup mechanism in a textured inlet of a hydrodynamic contact. *J Tribol* **130**(2): 021701 (2008)

[72] Rosenkranz A, Costa H L, Profito F, Gachot C, Medina S, Dini D. Influence of surface texturing on hydrodynamic friction in plane converging bearings—An experimental and numerical approach. *Tribol Int* **134**: 190–204 (2019)

[73] Tønder K. Dimpled pivoted plane bearings: Modified coefficients. *Tribol Int* **43**(12): 2303–2307 (2010)

[74] Tønder K. Micro- and macro-modifications of pivoted slider bearings: Performance comparison and texturing versus width reduction. *Tribol Int* **44**(4): 463–467 (2011)

[75] Papadopoulos C I, Efstathiou E E, Nikolakopoulos P G, Kaiktsis L. Geometry optimization of textured 3-D micro-thrust bearings. In *Proceedings of the ASME 2011 Turbo Expo: Turbine Technical Conference and Exposition*, Vancouver, Canada, 2012: 801–810.

[76] Papadopoulos C I, Nikolakopoulos P G, Kaiktsis L. Characterization of stiffness and damping in textured sector pad micro thrust bearings using computational fluid dynamics. *J Eng Gas Turbines Power* **134**(11): 112502 (2012)

[77] Gropper D, Harvey T J, Wang L. Numerical analysis and optimization of surface textures for a tilting pad thrust bearing. *Tribol Int* **124**: 134–144 (2018)

[78] Tala-Ighil N, Maspeyrot P, Fillon M, Bounif A. Effects of surface texture on journal-bearing characteristics under steady-state operating conditions. *Proc Inst Mech Eng Part J J Eng Tribol* **221**(6): 623–633 (2007)

[79] Tala-Ighil N, Fillon M, Maspeyrot P. Effect of textured area on the performances of a hydrodynamic journal bearing. *Tribol Int* **44**(3): 211–219 (2011)

[80] Cupillard S, Glavatskih S, Cervantes M J. Computational fluid dynamics analysis of a journal bearing with surface texturing. *Proc Inst Mech Eng Part J J Eng Tribol* **222**(2): 97–107 (2008)

[81] Brizmer V, Kligerman Y. A laser surface textured journal bearing. *J Tribol* **134**(3): 031702 (2012)

[82] Kango S, Sharma R K, Pandey R K. Thermal analysis of microtextured journal bearing using non-Newtonian rheology of lubricant and JFO boundary conditions. *Tribol Int* **69**: 19–29 (2014)

[83] Kango S, Sharma R K, Pandey R K. Comparative analysis of textured and grooved hydrodynamic journal bearing. *Proc Inst Mech Eng Part J J Eng Tribol* **228**(1): 82–95 (2014)

[84] Lu X B, Khonsari M M. An experimental investigation of dimple effect on the stribeck curve of journal bearings. *Tribol Lett* **27**(2): 169–176 (2007)

[85] Chen C, Wang X J, Shen Y F, Li Z L, Dong J. Experimental investigation for vibration reduction of surface-textured journal bearings. *Ind Lubr Tribol* **71**(2): 232–241 (2019)

[86] Yamada H, Taura H, Kaneko S. Static characteristics of journal bearings with square dimples. *J Tribol* **139**(5): 051703 (2017)

[87] Yamada H, Taura H, Kaneko S. Numerical and experimental analyses of the dynamic characteristics of journal bearings with square dimples. *J Tribol* **140**(1): 011703 (2018)

[88] Zhang X Y, Liu C P, Zhao B. An optimization research on groove textures of a journal bearing using particle swarm optimization algorithm. *Mech Ind* **22**: 1 (2021)

[89] Codrignani A, Savio D, Pastewka L, Frohnapfel B, van Ostayen R. Optimization of surface textures in hydrodynamic lubrication through the adjoint method. *Tribol Int* **148**: 106352 (2020)

[90] Costa H L, Hutchings I M. Hydrodynamic lubrication of textured steel surfaces under reciprocating sliding conditions. *Tribol Int* **40**(8): 1227–1238 (2007)

[91] Etsion I. State of the art in laser surface texturing. *J Tribol* **127**(1): 248–253 (2005)

[92] Wang X L, Wang J Q, Zhang B, Huang W. Design principles for the area density of dimple patterns. *Proc Inst Mech Eng Part J J Eng Tribol* **229**(4): 538–546 (2015)

[93] Wang X L, Kato K, Adachi K, Aizawa K. The effect of laser texturing of SiC surface on the critical load for the transition of water lubrication mode from hydrodynamic to mixed. *Tribol Int* **34**(10): 703–711 (2001)

[94] Fowell M T, Medina S, Olver A V, Spikes H A, Pegg I G. Parametric study of texturing in convergent bearings. *Tribol Int* **52**: 7–16 (2012)

[95] Cusano C, Wedeven L D. The effects of artificially-produced defects on the film thickness distribution in sliding EHD point contacts. *J Lubr Technol* **104**(3): 365–375 (1982)

[96] Wedeven L D, Cusano C. Elastohydrodynamic film thickness measurements of artificially produced surface dents and grooves. *A S L E Trans* **22**(4): 369–381 (1979)

[97] Ai X L, Cheng H S. The influence of moving dent on point EHL contacts. *Tribol Trans* **37**(2): 323–335 (1994)

[98] Kaneta M, Nishikawa H. Local reduction in thickness of point contact EHL films caused by a transversely oriented moving groove and its recovery. *J Tribol* **116**(3): 635–639 (1994)

[99] Mourier L, Mazuyer D, Lubrecht A A, Donnet C. Transient increase of film thickness in micro-textured EHL contacts. *Tribol Int* **39**(12): 1745–1756 (2006)

[100] Mourier L, Mazuyer D, Ninove F P, Lubrecht A A. Lubrication mechanisms with laser-surface-textured surfaces in elastohydrodynamic regime. *Proc Inst Mech Eng Part J J Eng Tribol* **224**(8): 697–711 (2010)

[101] Křupka I, Hartl M. Experimental study of microtextured surfaces operating under thin-film EHD lubrication conditions. *J Tribol* **129**(3): 502–508 (2007)

[102] Křupka I, Hartl M. The effect of surface texturing on thin EHD lubrication films. *Tribol Int* **40**(7): 1100–1110 (2007)

[103] Křupka I, Hartl M. Effect of surface texturing on very thin film EHD lubricated contacts. *Tribol Trans* **52**(1): 21–28 (2008)

[104] Křupka I, Hartl M, Svoboda P. Effects of surface topography on lubrication film formation within elastohydrodynamic and mixed lubricated non-conformal contacts. *Proc Inst Mech Eng Part J J Eng Tribol* **224**(8): 713–722 (2010)

[105] Křupka I, Vrbka M, Hartl M. Effect of surface texturing on mixed lubricated non-conformal contacts. *Tribol Int* **41**(11): 1063–1073 (2008)

[106] Vrbka M, Šamánek O, Šperka P, Návrat T, Křupka I, Hartl M. Effect of surface texturing on rolling contact fatigue within mixed lubricated non-conformal rolling/sliding contacts. *Tribol Int* **43**(8): 1457–1465 (2010)

[107] Ali F, Křupka I, Hartl M. Reducing the friction of lubricated nonconformal point contacts by transverse shallow micro-grooves. *Proc Inst Mech Eng Part J J Eng Tribol* **229**(4): 420–428 (2015)

[108] Ali F, Kaneta M, Křupka I, Hartl M. Experimental and numerical investigation on the behavior of transverse limited micro-grooves in EHL point contacts. *Tribol Int* **84**: 81–89 (2015)

[109] Křupka I, Hartl M, Zimmerman M, Houska P, Jang S. Effect of surface texturing on elastohydrodynamically lubricated contact under transient speed conditions. *Tribol Int* **44**(10): 1144–1150 (2011)

[110] Dumont M L, Lugt P M, Tripp J H. Surface feature effects in starved circular EHL contacts. *J Tribol* **124**(2): 358–366 (2002)

[111] Rosenkranz A, Heib T, Gachot C, Mücklich F. Oil film lifetime and wear particle analysis of laser-patterned stainless steel surfaces. *Wear* **334–335**: 1–12 (2015)

[112] Rosenkranz A, Szurdak A, Gachot C, Hirt G, Mücklich F. Friction reduction under mixed and full film EHL induced by hot micro-coined surface patterns. *Tribol Int* **95**: 290–297 (2016)

[113] Pettersson U, Jacobson S. Friction and wear properties of micro textured DLC coated surfaces in boundary lubricated sliding. *Tribol Lett* **17**(3): 553–559 (2004)

[114] Pettersson U, Jacobson S. Textured surfaces in sliding boundary lubricated contacts—Mechanisms, possibilities and limitations. *Tribol Mater Surf Interfaces* **1**(4): 181–189 (2007)

[115] Pettersson U, Jacobson S. Influence of surface texture on boundary lubricated sliding contacts. *Tribol Int* **36**(11): 857–864 (2003)

[116] Wang W Z, Huang Z X, Shen D, Kong L J, Li S S. The effect of triangle-shaped surface textures on the performance of the lubricated point-contacts. *J Tribol* **135**(2): 021503 (2013)

[117] Andersson P, Koskinen J, Varjus S, Gerbig Y, Haefke H, Georgiou S, Zhmud B, Buss W. Microlubrication effect by laser-textured steel surfaces. *Wear* **262**(3–4): 369–379 (2007)

[118] Kovalchenko A, Ajayi O, Erdemir A, Fenske G. Friction and wear behavior of laser textured surface under lubricated initial point contact. *Wear* **271**(9–10): 1719–1725 (2011)

[119] Nakatsuji T, Mori A. The tribological effect of mechanically produced micro-dents by a micro diamond pyramid on medium carbon steel surfaces in rolling–sliding contact. *Meccanica* **36**(6): 663–674 (2001)

[120] Zhai X J, Chang L, Hoeprich M R, Nixon H P. On mechanisms of fatigue life enhancement by surface dents in heavily loaded rolling line contacts. *Tribol Trans* **40**(4): 708–714 (1997) (in German)

[121] Mayer J. *Einfluss der Oberfläche und des Schmierstoffs auf das Reibungsverhalten im EHD-Kontakt.* München (Germany): Verl. Dr. Hut, 2014.

[122] Zhao J X, Sadeghi F. The effects of a stationary surface pocket on EHL line contact start-up. *J Tribol* **126**(4): 672–680 (2004)

[123] Bobzin K, Brögelmann T, Stahl K, Michaelis K, Mayer J, Hinterstoißer M. Friction reduction of highly-loaded rolling–sliding contacts by surface modifications under elasto-hydrodynamic lubrication. *Wear* **328–329**: 217–228 (2015)

[124] Pausch M. Untersuchung des Einflusses von Definiert Gefertigten Mikrostrukturen auf Schmierfilmbildung und

Kontaktpressung in Hoch belasteten Wälzkontakten. Ph.D. Thesis. Erlangen (Germany): Friedrich-Alexander-Universität Erlangen-Nürnberg, 2013. (in German)

[125] Wang W Z, Shen D, Zhang S G, Zhao Z Q. Investigation of patterned textures in ball-on-disk lubricated point contacts. *J Tribol* **137**(1): 011502 (2015)

[126] Weschta M. Untersuchungen zur Wirkungsweise von Mikrotexturen in Elastohydrodynamischen Gleit/Wälzkontakten. Ph.D. Thesis. Erlangen (Germany): Friedrich-Alexander-Universität Erlangen-Nürnberg, 2018. (in German)

[127] Shi X J, Wang L Q, Qin F Q. Relative fatigue life prediction of high-speed and heavy-load ball bearing based on surface texture. *Tribol Int* **101**: 364–374 (2016)

[128] Akamatsu Y, Tsushima N, Goto T, Hibi K. Influence of surface roughness skewness on rolling contact fatigue life. *Tribol Trans* **35**(4): 745–750 (1992)

[129] Gangopadhyay A, McWatt D G. The effect of novel surface textures on tappet shims on valvetrain friction and wear. *Tribol Trans* **51**(2): 221–230 (2008)

[130] Gupta N, Tandon N, Pandey R K. An exploration of the performance behaviors of lubricated textured and conventional spur gearsets. *Tribol Int* **128**: 376–385 (2018)

[131] Huang W, Wang X L. Biomimetic design of elastomer surface pattern for friction control under wet conditions. *Bioinspir Biomim* **8**(4): 046001 (2013)

[132] Kang Z Y, Fu Y H, Ji J H, Puoza J C. Effect of local laser surface texturing on tribological performance of injection cam. *Int J Adv Manuf Technol* **92**(5–8): 1751–1760 (2017)

[133] Marian M, Grützmacher P, Rosenkranz A, Tremmel S, Mücklich F, Wartzack S. Designing surface textures for EHL point-contacts—Transient 3D simulations, meta-modeling and experimental validation. *Tribol Int* **137**: 152–163 (2019)

[134] Marian M, Tremmel S, Wartzack S. Microtextured surfaces in higher loaded rolling–sliding EHL line-contacts. *Tribol Int* **127**: 420–432 (2018)

[135] Marian M, Weikert T, Tremmel S. On friction reduction by surface modifications in the TEHL cam/tappet-contact-experimental and numerical studies. *Coatings* **9**(12): 843 (2019)

[136] Marian M, Weschta M, Tremmel S, Wartzack S. Simulation of microtextured surfaces in starved EHL contacts using commercial FE software. *Matls Perf Charact* **6**(2): 165–181 (2017)

[137] Tremmel S, Marian M, Zahner M, Wartzack S, Merklein M. Friction reduction in EHL contacts by surface microtexturing—Tribological performance, manufacturing and tailored design. *Ind Lubr Tribol* **71**(8): 986–990 (2019)

[138] De La Guerra Ochoa E, Echávarri Otero J, Chacón Tanarro E, Lafont Morgado P, Díaz Lantada A, Munoz-Guijosa J M, Muñoz Sanz J L. Optimising lubricated friction coefficient by surface texturing. *Proc Inst Mech Eng C J Mech Eng Sci* **227**(11): 2610–2619 (2013)

[139] Boidi G, Da Silva M R, Profito F J, Machado I F. Using machine learning radial basis function (RBF) method for predicting lubricated friction on textured and porous surfaces. *Surf Topogr*: *Metrol Prop* **8**(4): 044002 (2020)

[140] Marian M. Numerische Auslegung von Oberflächenmikrotexturen für geschmierte tribologische Kontakte. Ph.D. Thesis. Erlangen (Germany): Friedrich-Alexander-Universität Erlangen-Nürnberg, 2021. (in German)

[141] Hadinata P C, Stephens L S. Soft elastohydrodynamic analysis of radial lip seals with deterministic microasperities on the shaft. *J Tribol* **129**(4): 851–859 (2007)

[142] Shinkarenko A, Kligerman Y, Etsion I. The effect of elastomer surface texturing in soft elasto-hydrodynamic lubrication. *Tribol Lett* **36**(2): 95–103 (2009)

[143] Shinkarenko A, Kligerman Y, Etsion I. The effect of surface texturing in soft elasto-hydrodynamic lubrication. *Tribol Int* **42**(2): 284–292 (2009)

[144] Shinkarenko A, Kligerman Y, Etsion I. The validity of linear elasticity in analyzing surface texturing effect for elastohydrodynamic lubrication. *J Tribol* **131**(2): 021503 (2009)

[145] Warren K H, Stephens L S. Effect of shaft microcavity patterns for flow and friction control on radial lip seal performance—A feasibility study. *Tribol Trans* **52**(6): 731–743 (2009)

[146] Li W, Stephens L S, Wenk J F. Experimental benchmarking of the numerical model of a radial lip seal with a surface textured shaft. *Tribol Trans* **56**(1): 75–87 (2013)

[147] Ito H, Kaneda K, Yuhta T, Nishimura I, Yasuda K, Matsuno T. Reduction of polyethylene wear by concave dimples on the frictional surface in artificial hip joints. *J Arthroplasty* **15**(3): 332–338 (2000)

[148] Chyr A, Qiu M F, Speltz J W, Jacobsen R L, Sanders A P, Raeymaekers B. A patterned microtexture to reduce friction and increase longevity of prosthetic hip joints. *Wear* **315**(1–2): 51–57 (2014)

[149] Sawano H, Warisawa S, Ishihara S. Study on long life of artificial joints by investigating optimal sliding surface geometry for improvement in wear resistance. *Precis Eng* **33**(4): 492–498 (2009)

[150] Gao L M, Hua Z K, Hewson R, Andersen M S, Jin Z M. Elastohydrodynamic lubrication and wear modelling of the knee joint replacements with surface topography. *Biosurface*

Biotribology **4**(1): 18–23 (2018)

[151] Dougherty P S M, Srivastava G, Onler R, Ozdoganlar O B, Higgs C F. Lubrication enhancement for UHMWPE sliding contacts through surface texturing. *Tribol Trans* **58**(1): 79–86 (2015)

[152] Dong Y C, Svoboda P, Vrbka M, Kostal D, Urban F, Cizek J, Roupcova P, Dong H S, Křupka I, Hartl M. Towards near-permanent CoCrMo prosthesis surface by combining micro-texturing and low temperature plasma carburising. *J Mech Behav Biomed Mater* **55**: 215–227 (2015)

[153] Hsu C J, Stratmann A, Rosenkranz A, Gachot C. Enhanced growth of ZDDP-based tribofilms on laser-interference patterned cylinder roller bearings. *Lubricants* **5**(4): 39 (2017)

[154] Boidi G, Tertuliano I S, Profito F J, De Rossi W, Machado I F. Effect of laser surface texturing on friction behaviour in elastohydrodynamically lubricated point contacts under different sliding-rolling conditions. *Tribol Int* **149**: 105613 (2020)

[155] Reynolds O. IV. On the theory of lubrication and its application to Mr. Beauchamp tower's experiments, including an experimental determination of the viscosity of olive oil. In *Philosophical Transactions of the Royal Society of London*. London: Royal Society, 1886: 157–234.

[156] Dowson D. A generalized Reynolds equation for fluid-film lubrication. *Int J Mech Sci* **4**(2): 159–170 (1962)

[157] Najji B, Bou-Said B, Berthe D. New formulation for lubrication with non-Newtonian fluids. *J Tribol* **111**(1): 29–34 (1989)

[158] Yang P R, Wen S Z. A generalized Reynolds equation for non-Newtonian thermal elastohydrodynamic lubrication. *J Tribol* **112**(4): 631–636 (1990)

[159] Sahlin F, Glavatskih S B, Almqvist T, Larsson R. Two-dimensional CFD-analysis of micro-patterned surfaces in hydrodynamic lubrication. *J Tribol* **127**(1): 96–102 (2005)

[160] Almqvist T, Larsson R. Some remarks on the validity of Reynolds equation in the modeling of lubricant film flows on the surface roughness scale. *J Tribol* **126**(4): 703–710 (2004)

[161] Almqvist A, Burtseva E, Rajagopal K, Wall P. On lower-dimensional models in lubrication, Part A: Common misinterpretations and incorrect usage of the Reynolds equation. *Proc Inst Mech Eng Part J J Eng Tribol* **235**(8): 1692–1702 (2021)

[162] Van Odyck D E A, Venner C H. Stokes flow in thin films. *J Tribol* **125**(1): 121–134 (2003)

[163] Wen C W, Meng X H, Li W X. Numerical analysis of textured piston compression ring conjunction using two-dimensional-computational fluid dynamics and Reynolds methods. *Proc Inst Mech Eng Part J J Eng Tribol* **232**(11): 1467–1485 (2018)

[164] Feldman Y, Kligerman Y, Etsion I, Haber S. The validity of the Reynolds equation in modeling hydrostatic effects in gas lubricated textured parallel surfaces. *J Tribol* **128**(2): 345–350 (2006)

[165] Etsion I. Modeling of surface texturing in hydrodynamic lubrication. *Friction* **1**(3): 195–209 (2013)

[166] Sommerfeld A. Zur Hydrodynamischen Theorie der Schmiermittelreibung. *Z Angew Math U Physik* **50**: 97–155 (1904) (in German)

[167] Paranjpe R S, Goenka P K. Analysis of crankshaft bearings using a mass conserving algorithm. *Tribol Trans* **33**(3): 333–344 (1990)

[168] Braun M J, Hannon W M. Cavitation formation and modelling for fluid film bearings: A review. *Proc Inst Mech Eng Part J J Eng Tribol* **224**(9): 839–863 (2010)

[169] Ausas R F, Jai M, Buscaglia G C. A mass-conserving algorithm for dynamical lubrication problems with cavitation. *J Tribol* **131**(3): 031702 (2009)

[170] Gümbel L. Vergleich der egebnisse der rechnerischen behandlung des lagerschmierungsproblem mit neueren versuchsergebnissen. *Mbl berl Bez VDI*: 125–128 (1921) (in German)

[171] Swift H W. The stability of lubricating films in journal bearings. *Minutes of the Proceedings of the Institution of Civil Engineers* **233**(1932): 267–288 (1932).

[172] Stieber W. *Hydrodynamische Theorie des Gleitlagers Das Schwimmlager*. Berlin (Germany): Verein Deutscher Ingenieure, 1933. (in German)

[173] Christopherson D G. A new mathematical method for the solution of film lubrication problems. *Proc Inst Mech Eng* **146**(1): 126–135 (1941)

[174] Venner C H, Lubrecht A A. *Multilevel Methods in Lubrication*. Amsterdam (the Netherlands): Elsevier Science, 2000.

[175] Murty K G. *Linear Complementarity, Linear and Nonlinear Programming*. Berlin (Germany): Heldermann Verlag, 1988.

[176] Wu S R. A penalty formulation and numerical approximation of the Reynolds–Hertz problem of elastohydrodynamic lubrication. *Int J Eng Sci* **24**(6): 1001–1013 (1986)

[177] Jakobsson B, Floberg L. *The Finite Journal Bearing, Considering Vaporization*. Göteborg (Sweden): Gumperts, 1957.

[178] Olsson K O. *Cavitation in Dynamically Loaded Bearings*. Göteborg (Sweden): Gumperts, 1965.

[179] Floberg L. *On Journal Bearing Lubrication Considering the Tensile Strength of the Liquid Lubricant*. Lund (Sweden): Machine Elements Division, Lund Technical University, 1973.

[180] Elrod H G. A cavitation algorithm. *J Lubr Technol* **103**(3): 350–354 (1981)

[181] Elrod H G, Adams M L. A computer program for cavitation and starvation problems. *Cavitation and Related Phenomena in Lubrication* **1**: 37–43 (1975)

[182] Vijayaraghavan D, Keith Jr T G. Development and evaluation of a cavitation algorithm. *Tribol Trans* **32**(2): 225–233 (1989)

[183] Vijayaraghavan D, Keith Jr T G. An efficient, robust, and time accurate numerical scheme applied to a cavitation algorithm. *J Tribol* **112**(1): 44–51 (1990)

[184] Sahlin F, Almqvist A, Larsson R, Glavatskih S. A cavitation algorithm for arbitrary lubricant compressibility. *Tribol Int* **40**(8): 1294–1300 (2007)

[185] Almqvist A, Fabricius J, Larsson R, Wall P. A new approach for studying cavitation in lubrication. *J Tribol* **136**(1): 011706 (2014)

[186] Bertocchi L, Dini D, Giacopini M, Fowell M T, Baldini A. Fluid film lubrication in the presence of cavitation: A mass-conserving two-dimensional formulation for compressible, piezoviscous and non-Newtonian fluids. *Tribol Int* **67**: 61–71 (2013)

[187] Almqvist A, Wall P. Modelling cavitation in (elasto)hydrodynamic lubrication. In *Advances in Tribology*. Darji P H, Ed. London: InTech, 2016: 197–213.

[188] Giacopini M, Fowell M T, Dini D, Strozzi A. A mass-conserving complementarity formulation to study lubricant films in the presence of cavitation. *J Tribol* **132**(4): 041702 (2010)

[189] Amendola M, De Moura C A, Zago J V, Pulino P, Gomes Neto F D A M. Numerical simulation of the cavitation in the hydrodynamic lubrication of journal bearings: A parallel algorithm. *J Braz Soc Mech Sci* **23**(3): 335–345 (2001)

[190] Ausas R, Ragot P, Leiva J, Jai M, Bayada G, Buscaglia G C. The impact of the cavitation model in the analysis of microtextured lubricated journal bearings. *J Tribol* **129**(4): 868–875 (2007)

[191] Bayada G, Chambat M, El Alaoui M. Variational formulations and finite element algorithms for cavitation problems. *J Tribol* **112**(2): 398–403 (1990)

[192] Tønder K, Christensen H. Waviness and roughness in hydrodynamic lubrication. *Proc Inst Mech Eng* **186**(1): 807–812 (1972)

[193] Teale J L, Lebeck A O. An evaluation of the average flow model [1] for surface roughness effects in lubrication. *J Lubr Technol* **102**(3): 360–366 (1980)

[194] Patir N, Cheng H S. An average flow model for determining effects of three-dimensional roughness on partial hydrodynamic lubrication. *J Lubr Technol* **100**(1): 12–17 (1978)

[195] Patir N, Cheng H S. Application of average flow model to lubrication between rough sliding surfaces. *J Lubr Technol* **101**(2): 220–229 (1979)

[196] Pérez-Ràfols F, Larsson R, Almqvist A. Modelling of leakage on metal-to-metal seals. *Tribol Int* **94**: 421–427 (2016)

[197] Pérez-Ràfols F, Larsson R, Lundström S, Wall P, Almqvist A. A stochastic two-scale model for pressure-driven flow between rough surfaces. *Proc Math Phys Eng Sci* **472**(2190): 20160069 (2016)

[198] Pérez-Ràfols F, Larsson R, Van Riet E J, Almqvist A. On the loading and unloading of metal-to-metal seals: A two-scale stochastic approach. *Proc Inst Mech Eng Part J J Eng Tribol* **232**(12): 1525–1537 (2018)

[199] Almqvist A, Essel E K, Fabricius J, Wall P. Reiterated homogenization applied in hydrodynamic lubrication. *Proc Inst Mech Eng Part J J Eng Tribol* **222**(7): 827–841 (2008)

[200] Lagemann V. *Numerische Verfahren zur tribologischen Charakterisierung bearbeitungsbedingter rauher Oberflächen bei Mikrohydrodynamik und Mischreibung*. Kassel (Germany): Univ.-Bibliothek, 2000. (in German)

[201] Scaraggi M. Lubrication of textured surfaces: A general theory for flow and shear stress factors. *Phys Rev E* **86**(2): 026314 (2012)

[202] Scaraggi M. Textured surface hydrodynamic lubrication: Discussion. *Tribol Lett* **48**(3): 375–391 (2012)

[203] Scaraggi M. Optimal textures for increasing the load support in a thrust bearing pad geometry. *Tribol Lett* **53**(1): 127–143 (2014)

[204] Rom M, Muller S. A reduced basis method for the homogenized Reynolds equation applied to textured surfaces. *Commun Comput Phys* **24**(2): 481–509 (2018)

[205] Rom M, Müller S. A new model for textured surface lubrication based on a modified Reynolds equation including inertia effects. *Tribol Int* **133**: 55–66 (2019)

[206] Waseem A, Temizer İ, Kato J, Terada K. Homogenization-based design of surface textures in hydrodynamic lubrication. *Int J Numer Methods Eng* **108**(12): 1427–1450 (2016)

[207] Waseem A, Temizer İ, Kato J, Terada K. Micro-texture design and optimization in hydrodynamic lubrication via two-scale analysis. *Struct Multidiscip Optim* **56**(2): 227–248 (2017)

[208] Yıldıran İ N, Temizer İ, Çetin B. Homogenization in hydrodynamic lubrication: Microscopic regimes and re-entrant textures. *J Tribol* **140**(1): 011701 (2018)

[209] Spencer A, Almqvist A, Larsson R. A semi-deterministic texture-roughness model of the piston ring–cylinder liner contact. *Proc Inst Mech Eng Part J J Eng Tribol* **225**(6): 325–333 (2011)

[210] Söderfjäll M, Larsson R, Marklund P, Almqvist A. Texture-induced effects causing reduction of friction in mixed lubrication for twin land oil control rings. *Proc Inst Mech Eng Part J J Eng Tribol* **232**(2): 166–178 (2018)

[211] Greenwood J A, Williamson J B P. Contact of nominally flat surfaces. *Proc Roy Soc A Math Phy* **295**(1442): 300–319 (1966)

[212] Greenwood J A, Tripp J H. The elastic contact of rough spheres. *J Appl Mech* **34**(1): 153–159 (1967)

[213] Bush A W, Gibson R D, Thomas T R. The elastic contact of a rough surface. *Wear* **35**(1): 87–111 (1975)

[214] McCool J I. Comparison of models for the contact of rough surfaces. *Wear* **107**(1): 37–60 (1986)

[215] Greenwood J A, Tripp J H. The contact of two nominally flat rough surfaces. *Proc Inst Mech Eng* **185**(1): 625–633 (1970)

[216] Chang W R, Etsion I, Bogy D B. An elastic–plastic model for the contact of rough surfaces. *J Tribol* **109**(2): 257–263 (1987)

[217] Halling J, Nuri K A. Elastic/plastic contact of surfaces considering ellipsoidal asperities of work-hardening multi-phase materials. *Tribol Int* **24**(5): 311–319 (1991)

[218] Jamari J, Schipper D J. An elastic–plastic contact model of ellipsoid bodies. *Tribol Lett* **21**(3): 262–271 (2006)

[219] Zhao Y W, Maietta D M, Chang L. An asperity microcontact model incorporating the transition from elastic deformation to fully plastic flow. *J Tribol* **122**(1): 86–93 (2000)

[220] Müser M H, Dapp W B, Bugnicourt R, Sainsot P, Lesaffre N, Lubrecht T A, Persson B N J, Harris K, Bennett A, Schulze K, et al. Meeting the contact-mechanics challenge. *Tribol Lett* **65**(4): 118 (2017)

[221] Persson B N J. Theory of rubber friction and contact mechanics. *J Chem Phys* **115**(8): 3840–3861 (2001)

[222] Prodanov N, Dapp W B, Müser M H. On the contact area and mean gap of rough, elastic contacts: Dimensional analysis, numerical corrections, and reference data. *Tribol Lett* **53**(2): 433–448 (2014)

[223] Kogut L, Etsion I. Elastic–plastic contact analysis of a sphere and a rigid flat. *J Appl Mech* **69**(5): 657–662 (2002)

[224] Kogut L, Etsion I. A finite element based elastic–plastic model for the contact of rough surfaces. *Tribol Trans* **46**(3): 383–390 (2003)

[225] Kogut L, Etsion I. A static friction model for elastic–plastic contacting rough surfaces. *J Tribol* **126**(1): 34–40 (2004)

[226] Jackson R L, Green I. A finite element study of elasto–plastic hemispherical contact against a rigid flat. *J Tribol* **127**(2): 343–354 (2005)

[227] Jackson R L, Green I. A statistical model of elasto–plastic asperity contact between rough surfaces. *Tribol Int* **39**(9): 906–914 (2006)

[228] Sahlin F, Larsson R, Almqvist A, Lugt P M, Marklund P. A mixed lubrication model incorporating measured surface topography. Part 1: Theory of flow factors. *Proc Inst Mech Eng Part J J Eng Tribol* **224**(4): 335–351 (2010)

[229] Sahlin F, Larsson R, Marklund P, Almqvist A, Lugt P M. A mixed lubrication model incorporating measured surface topography. Part 2: Roughness treatment, model validation, and simulation. *Proc Inst Mech Eng Part J J Eng Tribol* **224**(4): 353–365 (2010)

[230] Bartel D. *Simulation von Tribosystemen: Grundlagen und Anwendungen*. Wiesbaden (Germany): Vieweg+Teubner, 2010. (in German)

[231] Carslaw H S, Jaeger J C. *Conduction of Heat in Solids,* 2nd edn. Oxford (UK): Clarendon Press, 1959.

[232] Häfner F, Sames D, Voigt H D. *Wärme- und Stofftransport: Mathematische Methoden*. Berlin: Springer Lehrbuch, 1992.

[233] Jaeger J C. Moving sources of heat and the temperature at sliding contacts. *Journal Proceedings of the Royal Society of New South Wales* **76**: 203–224 (1942)

[234] Qiu L H, Cheng H S. Temperature rise simulation of three-dimensional rough surfaces in mixed lubricated contact. *J Tribol* **120**(2): 310–318 (1998)

[235] Zhao J X, Sadeghi F, Hoeprich M H. Analysis of EHL circular contact start up: Part II—Surface temperature rise model and results. *J Tribol* **123**(1): 75–82 (2001)

[236] Gasch R, Knothe K. *Strukturdynamik: Band 2: Kontinua und ihre Diskretisierung*. Berlin: Springer Berlin, Heidelberg, 1989. (in German)

[237] Charitopoulos A, Fillon M, Papadopoulos C I. Numerical investigation of parallel and quasi-parallel slider bearings operating under thermoelastohydrodynamic (TEHD) regime. *Tribol Int* **149**: 105517 (2020)

[238] Chalkiopoulos M, Charitopoulos A, Fillon M, Papadopoulos C I. Effects of thermal and mechanical deformations on textured thrust bearings optimally designed by a THD calculation method. *Tribol Int* **148**: 106303 (2020)

[239] Bruyere V, Fillot N, Morales-Espejel G E, Vergne P. Computational fluid dynamics and full elasticity model for sliding line thermal elastohydrodynamic contacts. *Tribol Int* **46**(1): 3–13 (2012)

[240] Hartinger M, Dumont M L, Ioannides S, Gosman D, Spikes H. CFD modeling of a thermal and shear-thinning elastohydrodynamic line contact. *J Tribol* **130**(4): 041503 (2008)

[241] Hartinger M, Gosman D, Ioannides S, Spikes H A. CFD Modelling of Elastohydrodynamic Lubrication. In *Proceedings of the World Tribology Congress III*, Washington D.C., USA, 2005: 531–532.

[242] Almqvist T, Almqvist A, Larsson R. A comparison between computational fluid dynamic and Reynolds approaches for simulating transient EHL line contacts. *Tribol Int* **37**(1): 61–69 (2004)

[243] Mohrenstein-Ertel A. *Die Berechnung der Hydrodynamischen Schmierung Gekrümmter Oberflächen unter Hoher Belastung und Relativbewegung*. Düsseldorf (Germany): Verein Deutscher Ingenieure-Verlag, 1984. (in German)

[244] Dowson D, Higginson G R. A numerical solution to the elasto-hydrodynamic problem. *J Mech Eng Sci* **1**(1): 6–15 (1959)

[245] Evans H P, Snidle R W. Inverse solution of Reynolds' equation of lubrication under point-contact elastohydrodynamic conditions. *J Lubr Technol* **103**(4): 539–546 (1981)

[246] Hamrock B J, Dowson D. Isothermal elastohydrodynamic lubrication of point contacts: Part I—Theoretical formulation. *J Lubr Technol* **98**(2): 223–228 (1976)

[247] Hamrock B J, Dowson D. Isothermal elastohydrodynamic lubrication of point contacts: Part II—Ellipticity parameter results. *J Lubr Technol* **98**(3): 375–381 (1976)

[248] Hamrock B J, Dowson D. Isothermal elastohydrodynamic lubrication of point contacts: Part IV—Starvation results. *J Lubr Technol* **99**(1): 15–23 (1977)

[249] Hamrock B J, Dowson D. Isothermal elastohydrodynamic lubrication of point contacts: Part III—Fully flooded results. *J Lubr Technol* **99**(2): 264–275 (1977)

[250] Lubrecht A A. The numerical solution of the lubricated line- and point contact problem using multigrid techniques. Ph.D. Thesis. Enschede (the Netherlands): University of Twente, 1987.

[251] Venner C H, Napel W E T. Multilevel solution of the elastohydrodynamically lubricated circular contact problem part I: Theory and numerical algorithm. *Wear* **152**(2): 351–367 (1992)

[252] Venner C H, Napel W E T. Multilevel solution of the elastohydrodynamically lubricated circular contact problem part 2: Smooth surface results. *Wear* **152**(2): 369–381 (1992)

[253] Venner C H. Multilevel solution of the EHL line and point-contact problems. Ph.D. Thesis. Enschede (the Netherlands): University of Twente, 1991.

[254] Stanley H M, Kato T. An FFT-based method for rough surface contact. *J Tribol* **119**(3): 481–485 (1997)

[255] Ju Y, Farris T N. Spectral analysis of two-dimensional contact problems. *J Tribol* **118**(2): 320–328 (1996)

[256] Hu Y Z, Zhu D. A full numerical solution to the mixed lubrication in point contacts. *J Tribol* **122**(1): 1–9 (2000)

[257] Wang Q J, Zhu D. *Interfacial Mechanics: Theories and Methods for Contact and Lubrication.* New York: CRC Press, 2019.

[258] Rohde S M, Oh K P. A unified treatment of thick and thin film elastohydrodynamic problems by using higher order element methods. *Proc R Soc Lond A* **343**(1634): 315–331 (1975)

[259] Oh K P, Rohde S M. Numerical solution of the point contact problem using the finite element method. *Int J Numer Methods Eng* **11**(10): 1507–1518 (1977)

[260] Okamura H. A contribution to the numerical analysis of isothermal elastohydrodynamic lubrication. In *Proceedings of the 9th Leeds–Lyon Symposium on Tribology*, London, 1982.

[261] Habchi W, Eyheramendy D, Vergne P, Morales-Espejel G. A full-system approach of the elastohydrodynamic line/point contact problem. *J Tribol* **130**(2): 021501 (2008)

[262] Tan X C, Goodyer C E, Jimack P K, Taylor R I, Walkley M A. Computational approaches for modelling elastohydrodynamic lubrication using multiphysics software. *Proc Inst Mech Eng Part J J Eng Tribol* **226**(6): 463–480 (2012)

[263] Lohner T, Ziegltrum A, Stemplinger J P, Stahl K. Engineering software solution for thermal elastohydrodynamic lubrication using multiphysics software. *Adv Tribol* **2016**: 6507203 (2016)

[264] Habchi W. Coupling strategies for finite element modeling of thermal elastohydrodynamic lubrication problems. *J Tribol* **139**(4): 041501 (2017)

[265] Marian M, Weschta M, Tremmel S, Wartzack S. Einfluss masseerhaltender kavitationsmodelle bei der simulation hydro- und elastohydrodynamischer kontakte. *Tribologie und Schmierungstechnik* **64**(4): 29–34 (2017) (in German)

[266] Kaneta M, Shigeta T, Yang P R. Film pressure distributions in point contacts predicted by thermal EHL analyses. *Tribol Int* **39**(8): 812–819 (2006)

[267] Wang Y Q, Li H Q, Tong J W, Yang P R. Transient thermoelastohydrodynamic lubrication analysis of an involute spur gear. *Tribol Int* **37**(10): 773–782 (2004)

[268] Tremmel S, Marian M, Zahner M, Weschta M, Engel U, Wartzack S, Merklein M. Reibungsreduzierung in EHD-Kontakten durch mikrostrukturierte Bauteiloberflächen–Auslegung, Gestaltung und umformtechnische Herstellung. In: Gesellschaft für Tribologie e V, Ed. Göttingen (Germany): Sonderband Abschlusskolloquium Ressourceneffiziente Konstruktionselemente SPP 2017: 149–166. (in German)

[269] Zhu D, Hu Y Z. A computer program package for the prediction of EHL and mixed lubrication characteristics, friction, subsurface stresses and flash temperatures based on measured 3-D surface roughness. *Tribol Trans* **44**(3): 383–390 (2001)

[270] Evans H P, Snidle B W. Analysis of micro-elastohydrodynamic lubrication for engineering contacts. *Tribol Int* **29**(8): 659–667 (1996)

[271] De Boer G N, Almqvist A. On the two-scale modelling of elastohydrodynamic lubrication in tilted-pad bearings. *Lubricants* **6**(3): 78 (2018)

[272] De Boer G N, Gao L, Hewson R W, Thompson H M. Heterogeneous Multiscale Methods for modelling surface topography in elastohydrodynamic lubrication line contacts. *Tribol Int* **113**: 262–278 (2017)

[273] De Boer G N, Hewson R W, Thompson H M, Gao L, Toropov V V. Two-scale EHL: Three-dimensional topography in tilted-pad bearings. *Tribol Int* **79**: 111–125 (2014)

[274] Johnson K L, Greenwood J A, Poon S Y. A simple theory of asperity contact in elastohydro-dynamic lubrication. *Wear* **19**(1): 91–108 (1972)

[275] Masjedi M, Khonsari M M. Film thickness and asperity load formulas for line-contact elastohydrodynamic lubrication with provision for surface roughness. *J Tribol* **134**(1): 011503 (2012)

[276] Masjedi M, Khonsari M M. On the effect of surface roughness in point-contact EHL: Formulas for film thickness and asperity load. *Tribol Int* **82**: 228–244 (2015)

[277] Masjedi M, Khonsari M M. Mixed lubrication of soft contacts: An engineering look. *Proc Inst Mech Eng Part J J Eng Tribol* **231**(2): 263–273 (2017)

[278] Costa H L, Hutchings I M. Some innovative surface texturing techniques for tribological purposes. *Proc Inst Mech Eng Part J J Eng Tribol* **229**(4): 429–448 (2015)

[279] Vaeth K M, Jackman R J, Black A J, Whitesides G M, Jensen K F. Use of microcontact printing for generating selectively grown films of poly(p-phenylene vinylene) and parylenes prepared by chemical vapor deposition. *Langmuir* **16**(22): 8495–8500 (2000)

[280] Wang H Y, Wang Y Q, Xue R Z, Kang L P, Li X J. Fabrication and electron field-emission of carbon nanofibers grown on silicon nanoporous pillar array. *Appl Surf Sci* **261**: 219–222 (2012)

[281] Bartz M, Terfort A, Knoll W, Tremel W. Stamping of monomeric SAMs as a route to structured crystallization templates: Patterned titania films. *Chem Weinheim Der Bergstrasse Ger* **6**(22): 4149–4153 (2000)

[282] Deng T, Arias F, Ismagilov R F, Kenis P J A, Whitesides G M. Fabrication of metallic microstructures using exposed, developed silver halide-based photographic film. *Anal Chem* **72**(4): 645–651 (2000)

[283] Mott M, Evans J R G. Zirconia/alumina functionally graded material made by ceramic ink jet printing. *Mater Sci Eng A* **271**(1–2): 344–352 (1999)

[284] Lejeune M, Chartier T, Dossou-Yovo C, Noguera R. Ink-jet printing of ceramic micro-pillar arrays. *J Eur Ceram Soc* **29**(5): 905–911 (2009)

[285] Hutchings I M, Martin J D. *Inkjet Technology for Digital Fabrication*. Chichester (UK): John Wiley & Sons, 2013.

[286] Snell D, Coombs A. Novel coating technology for non-oriented electrical steels. *J Magn Magn Mater* **215–216**: 133–135 (2000)

[287] Kumar A V, Dutta A. Electrophotographic layered manufacturing. *J Manuf Sci Eng* **126**(3): 571–576 (2004)

[288] Nelson J B, Schwartz D T. Electrochemical printing: *In situ* characterization using an electrochemical quartz crystal microbalance. *J Micromech Microeng* **15**(12): 2479–2484 (2005)

[289] Zou M, Cai L, Wang H. Adhesion and friction studies of a nano-textured surface produced by spin coating of colloidal silica nanoparticle solution. *Tribol Lett* **21**(1): 25–30 (2006)

[290] Dumitru G, Romano V, Weber H P, Haefke H, Gerbig Y, Pflüger E. Laser microstructuring of steel surfaces for tribological applications. *Appl Phys A* **70**(4): 485–487 (2000)

[291] Geiger M, Roth S, Becker W. Influence of laser-produced microstructures on the tribological behaviour of ceramics. *Surf Coat Technol* **100–101**: 17–22 (1998)

[292] Semaltianos N G, Perrie W, French P, Sharp M, Dearden G, Watkins K G. Femtosecond laser surface texturing of a nickel-based superalloy. *Appl Surf Sci* **255**(5): 2796–2802 (2008)

[293] Vincent C, Monteil G, Barriere T, Gelin J C. Control of the quality of laser surface texturing. *Microsyst Technol* **14**(9–11): 1553–1557 (2008)

[294] Aspinwall D K, Wise M L H, Stout K J, Goh T H A, Zhao F L, El-Menshawy M F. Electrical discharge texturing. *Int J Mach Tools Manuf* **32**(1–2): 183–193 (1992)

[295] Langford R M, Dale G, Hopkins P J, Ewen P J S, Petford-Long A K. Focused ion beam micromachining of three-dimensional structures and three-dimensional reconstruction to assess their shape. *J Micromech Microeng* **12**(2): 111–114 (2002)

[296] Ike H. Properties of metal sheets with 3-D designed surface microgeometry prepared by special rolls. *J Mater Process Technol* **60**(1–4): 363–368 (1996)

[297] Zhang J Y, Meng Y G. A study of surface texturing of carbon steel by photochemical machining. *J Mater Process Technol* **212**(10): 2133–2140 (2012)

[298] Byun J W, Shin H S, Kwon M H, Kim B H, Chu C N. Surface texturing by micro ECM for friction reduction. *Int J Precis Eng Manuf* **11**(5): 747–753 (2010)

[299] Schönenberger I, Roy S. Microscale pattern transfer without photolithography of substrates. *Electrochimica Acta* **51**(5): 809–819 (2005)

[300] Costa H L, Hutchings I M. Development of a maskless electrochemical texturing method. *J Mater Process Technol* **209**(8): 3869–3878 (2009)

[301] Parreira J G, Gallo C A, Costa H L. New advances on maskless electrochemical texturing (MECT) for tribological purposes. *Surf Coat Technol* **212**: 1–13 (2012)

[302] Denkena B, Kästner J, Knoll G, Brandt S, Bach F W, Drößler B, et al. Mikrostrukturierung funktionaler oberflächen. *Werkstattstechnik Online* **98**(6): 486–494 (2008) (in German)

[303] Weck M, Fischer S, Vos M. Fabrication of microcomponents using ultraprecision machine tools. *Nanotechnology* **8**(3): 145–148 (1997)

[304] Tian H, Saka N, Suh N P. Boundary lubrication studies on undulated titanium surfaces. *Tribol Trans* **32**(3): 289–296 (1989)

[305] Slikkerveer P J, Veld F H I. Model for patterned erosion. *Wear* **233–235**: 377–386 (1999)

[306] Lasagni A, D'Alessandria M, Giovanelli R, Mücklich F. Advanced design of periodical architectures in bulk metals by means of laser interference metallurgy. *Appl Surf Sci* **254**(4): 930–936 (2007)

[307] Duarte M, Lasagni A, Giovanelli R, Narciso J, Louis E, Mücklich F. Increasing lubricant film lifetime by grooving periodical patterns using laser interference metallurgy. *Adv Eng Mater* **10**(6): 554–558 (2008)

[308] Mücklich F, Lasagni A, Daniel C. Laser Interference Metallurgy—Using interference as a tool for micro/nano structuring. *Int J Mater Res* **97**(10): 1337–1344 (2006)

[309] Lasagni A, Benke D, Kunze T, Bieda M, Eckhardt S, Roch T, Langheinrich D, Berger J. Bringing the direct laser interference patterning method to industry: A one tool-complete solution for surface functionalization. *J Laser Micro Nanoeng* **10**(3): 340–344 (2015)

[310] Hirt G, Thome M. Large area rolling of functional metallic micro structures. *Prod Eng* **1**(4): 351–356 (2007)

[311] Klocke F, Feldhaus B, Mader S. Development of an incremental rolling process for the production of defined riblet surface structures. *Prod Eng* **1**(3): 233–237 (2007)

[312] Engel U, Eckstein R. Microforming—From basic research to its realization. *J Mater Process Technol* **125–126**: 35–44 (2002)

[313] Szurdak A, Hirt G. Finite element analysis of manufacturing micro lubrication pockets in high strength steels by hot micro-coining. *Steel Res Int* **86**(3): 257–265 (2015)

[314] Szurdak A, Rosenkranz A, Gachot C, Hirt G, Mücklich F. Manufacturing and tribological investigation of hot micro-coined lubrication pockets. *Key Eng Mater* **611–612**: 417–424 (2014)

[315] Siebertz K, van Bebber D, Hochkirchen T. *Statistische Versuchsplanung: Design of Experiments (DoE)*. Berlin: Springer Vieweg, 2010.

[316] Booker A J, Dennis J E, Frank P D, Serafini D B, Torczon V, Trosset M W. A rigorous framework for optimization of expensive functions by surrogates. *Struct Optim* **17**(1): 1–13 (1999)

[317] Simpson T W, Poplinski J D, Koch P N, Allen J K. Metamodels for computer-based engineering design: Survey and recommendations. *Eng Comput* **17**(2): 129–150 (2001)

[318] Rosenkranz A, Marian M, Profito F J, Aragon N, Shah R. The use of artificial intelligence in tribology—A perspective. *Lubricants* **9**(1): 2 (2020)

[319] Marian M, Tremmel S. Current trends and applications of machine learning in tribology—A review. *Lubricants* **9**(9): 86 (2021)

[320] Kleppmann W. *Taschenbuch Versuchsplanung: Produkte und Prozesse Optimieren*. München (Germany): Hanser Verlag GmbH & Co. KG, 2009.

[321] Johnson M E, Moore L M, Ylvisaker D. Minimax and maximin distance designs. *J Stat Plan Inference* **26**(2): 131–148 (1990)

[322] Nocedal J, Wright S J. *Numerical Optimization*. New York: Springer, 2006.

[323] Box G E P, Wilson K B. On the experimental attainment of optimum conditions. *J Royal Stat Soc Ser B Methodol* **13**(1): 1–45 (1951)

[324] Box G E P, Draper N R. *Response Surfaces, Mixtures, and Ridge Analyses,* 2nd edn. New York: John Wiley & Sons, 2007.

[325] Eberhart R, Kennedy J. A new optimizer using particle swarm theory. In *MHS'95. Proceedings of the Sixth International Symposium on Micro Machine and Human Science*, Nagoya, Japan, 1995: 39–43.

[326] Weicker K. *Evolutionäre Algorithmen,* 3rd edn. Wiesbaden (Germany): Springer Vieweg, 2015.

[327] Kruse R, Borgelt C, Braune C, Klawonn F, Moewes C, Steinbrecher M. *Computational Intelligence: Eine methodische Einführung in künstliche neuronale Netze, evolutionäre Algorithmen, Fuzzy-Systeme und Bayes-Netze,* 2nd edn. Wiesbaden (Germany): Springer Vieweg; 2015. (in German)

[328] Alt W. Semi-local convergence of the Lagrange–Newton method with application to optimal control. In *Recent Developments in Optimization. Lecture Notes in Economics and Mathematical Systems, Vol 429*. Durier R., Michelot C. Eds. Berlin: Springer Berlin Heidelberg, 1–16.

[329] Wilson R B. A simplicial algorithm for concave programming. Ph.D. Thesis. Springs (USA): University of Colorado Colorado Springs, 1963.

[330] Sigmund O, Maute K. Topology optimization approaches. *Struct Multidiscip Optim* **48**(6): 1031–1055 (2013)

[331] Svanberg K. The method of moving asymptotes—A new method for structural optimization. *Int J Numer Methods Eng* **24**(2): 359–373 (1987)

[332] Svanberg K. A class of globally convergent optimization methods based on conservative convex separable approximations. *SIAM J Optim* **12**(2): 555–573 (2002)

[333] Almqvist A. A cavitation algorithm. Available on https://www.mathworks.com/matlabcentral/fileexchange/41484-a-cavitation-algorithm, 2016

[334] Zhang J Y, Meng Y G. Direct observation of cavitation phenomenon and hydrodynamic lubrication analysis of textured surfaces. *Tribol Lett* **46**(2): 147–158 (2012)

[335] Fowell M, Olver A V, Gosman A D, Spikes H A, Pegg I. Entrainment and inlet suction: Two mechanisms of hydrodynamic lubrication in textured bearings. *J Tribol* **129**(2): 336–347 (2007)

[336] Olver A V, Fowell M T, Spikes H A, Pegg I G. 'Inlet suction', a load support mechanism in non-convergent, pocketed, hydrodynamic bearings. *Proc Inst Mech Eng Part J J Eng Tribol* **220**(2): 105–108 (2006)

[337] Kovalchenko A, Ajayi O, Erdemir A, Fenske G, Etsion I. The effect of laser surface texturing on transitions in lubrication regimes during unidirectional sliding contact. *Tribol Int* **38**(3): 219–225 (2005)

[338] Kalliorinne K, Pérez-Ràfols F, Fabricius J, Almqvist A. Application of topological optimisation methodology to infinitely wide slider bearings operating under compressible flow. *Proc Inst Mech Eng Part J J Eng Tribol* **234**(7): 1035–1050 (2020)

[339] Kalliorinne K, Almqvist A. Application of topological optimisation methodology to finitely wide slider bearings operating under incompressible flow. *Proc Inst Mech Eng Part J J Eng Tribol* **235**(4): 698–710 (2021)

[340] Kalliorinne K, Larsson R, Almqvist A. Application of topological optimisation methodology to hydrodynamic thrust bearings. *Proc Inst Mech Eng Part J J Eng Tribol* **235**(8): 1669–1679 (2021)

[341] Rayleigh L. I. Notes on the theory of lubrication. *Lond Edinb Dublin Philos Mag J Sci* **35**(205): 1–12 (1918)

[342] Maday C J. A bounded variable approach to the optimum slider bearing. *J Lubr Technol* **90**(1): 240–242 (1968)

[343] Boldyrev Y Y. Periodic variational Rayleigh problem of the gas-film lubrication theory. *J Mach Manuf Reliab* **45**(4): 354–361 (2016)

[344] Auloge J Y, Bourgin P, Gay B. The optimum design of one-dimensional bearings with non-Newtonian lubricants. *J Lubr Technol* **105**(3): 391–395 (1983)

[345] Rohde S M. The optimum slider bearing in terms of friction. *J Lubr Technol* **94**(3): 275–279 (1972)

[346] Badescu V. Optimization of One Dimensional Slider Bearings. In *Optimal Control in Thermal Engineering*. Badescu V, Ed. Cham (Switzerland): Springer, 2017: 529–581.

[347] Fesanghary M, Khonsari M M. Topological and shape optimization of thrust bearings for enhanced load-carrying capacity. *Tribol Int* **53**: 12–21 (2012)

[348] Kettleborough C F. The hydrodynamic pocket thrust-bearing. *Proc Inst Mech Eng* **170**(1): 535–544 (1956)

[349] van Ostayen R A J. Film height optimization of dynamically loaded hydrodynamic slider bearings. *Tribol Int* **43**(10): 1786–1793 (2010)

[350] Dobrica M, Fillon M. Reynolds' model suitability in simulating Rayleigh step bearing thermohydrodynamic problems. *Tribol Trans* **48**(4): 522–530 (2005)

[351] Choo J W, Olver A V, Spikes H A. The influence of transverse roughness in thin film, mixed elastohydrodynamic lubrication. *Tribol Int* **40**(2): 220–232 (2007)

[352] Venner C H, Lubrecht A A. Numerical simulation of a transverse ridge in a circular EHL contact under rolling/sliding. *J Tribol* **116**(4): 751–761 (1994)

[353] Most T, Will J. Metamodel of optimal prognosis—An automatic approach for variable reduction and optimal meta-model selection. In *Proceedings of the Weimar Optimization and Stochastic Days 5.0*, Weinar, Germany, 2008.

[354] Most T, Will J. Recent advances in Meta-model of optimal prognosis. In *Proceedings of the Weimar Optimization and Stochastic Days 7.0*, Weinar, Germany, 2010: 21–22.

[355] Boidi G, Grützmacher P G, Varga M, Rodrigues da Silva M, Gachot C, Dini D, Profito F J, Machado I F. Tribological performance of random sinter pores vs. deterministic laser surface textures: An experimental and machine learning approach. In *Tribology*. Pintaude G, Cousseau T, Eds. London: IntechOpen, 2021.

[356] Ai X L. Effect of three-dimensional random surface roughness on fatigue life of a lubricated contact. *J Tribol* **120**(2): 159–164 (1998)

[357] Olver A V. The mechanism of rolling contact fatigue: An update. *Proc Inst Mech Eng Part J J Eng Tribol* **219**(5): 313–330 (2005)

[358] Deolalikar N, Sadeghi F. Fatigue life reduction in mixed lubricated elliptical contacts. *Tribol Lett* **27**(2): 197–209 (2007)

[359] Vrbka M, Křupka I, Šamánek O, Svoboda P, Vaverka M, Hartl M. Effect of surface texturing on lubrication film formation and rolling contact fatigue within mixed lubricated non-conformal contacts. *Meccanica* **46**(3): 491–498 (2011)

[360] Britton R D, Elcoate C D, Alanou M P, Evans H P, Snidle R W. Effect of surface finish on gear tooth friction. *J Tribol* **122**(1): 354–360 (2000)

[361] Beilicke R, Bobach L, Bartel D. Transient thermal elastohydrodynamic simulation of a DLC coated helical gear pair considering limiting shear stress behavior of the lubricant. *Tribol Int* **97**: 136–150 (2016)

[362] Ziegltrum A, Lohner T, Stahl K. TEHL simulation on the influence of lubricants on the frictional losses of DLC coated gears. *Lubricants* **6**(1): 17 (2018)

[363] Kano M. Super low friction of DLC applied to engine cam follower lubricated with ester-containing oil. *Tribol Int* **39**(12): 1682–1685 (2006)

[364] Gangopadhyay A, McWatt D G, Zdrodowski R J, Simko S J, Matera S, Sheffer K, Furby R S. Valvetrain friction reduction through thin film coatings and polishing. *Tribol Trans* **55**(1): 99–108 (2012)

[365] Dobrenizki L, Tremmel S, Wartzack S, Hoffmann D C, Brögelmann T, Bobzin K, Bagcivan N, Musayev Y, Hosenfeldt T. Efficiency improvement in automobile bucket tappet/camshaft contacts by DLC coatings—Influence of engine oil, temperature and camshaft speed. *Surf Coat Technol* **308**: 360–373 (2016)

[366] Shi F H, Salant R F. A mixed soft elastohydrodynamic lubrication model with interasperity cavitation and surface shear deformation. *J Tribol* **122**(1): 308–316 (2000)

[367] Shi F H, Salant R F. Numerical study of a rotary lip seal with a quasi-random sealing surface. *J Tribol* **123**(3): 517–524 (2001)

[368] Ghosh S, Abanteriba S. Status of surface modification techniques for artificial hip implants. *Sci Technol Adv Mater* **17**(1): 715–735 (2016)

[369] Shah R, Gashi B, Hoque S, Marian M, Rosenkranz A. Enhancing mechanical and biomedical properties of protheses—Surface and material design. *Surf Interfaces* **27**: 101498 (2021)

[370] Nečas D, Usami H, Niimi T, Sawae Y, Křupka I, Hartl M. Running-in friction of hip joint replacements can be significantly reduced: The effect of surface-textured acetabular cup. *Friction* **8**(6): 1137–1152 (2020)

[371] Marian M, Orgeldinger C, Rothammer B, Nečas D, Vrbka M, Křupka I, Hartl M, Wimmer M A, Tremmel S, Wartzack S. Towards the understanding of lubrication mechanisms in total knee replacements—Part II: Numerical modeling. *Tribol Int* **156**: 106809 (2021)

[372] Nečas D, Vrbka M, Marian M, Rothammer B, Tremmel S, Wartzack S, Galandáková A, Gallo J, Wimmer M A, Křupka I, et al. Towards the understanding of lubrication mechanisms in total knee replacements—Part I: Experimental investigations. *Tribol Int* **156**: 106874 (2021)

Max Marian. He is an assistant professor for multiscale engineering mechanics at the Department of Mechanical and Metallurgical Engineering of Pontificia Universidad Católica de Chile. His research focuses on energy efficiency and sustainability through tribology, with an emphasis on the modification of surfaces through micro-texturing and coatings. Besides machine elements and engine components, he expanded his fields towards biotribology and artificial joints. His research is particularly related to the development of numerical multiscale tribo-simulation and machine learning approaches. He has published more than 30 peer-reviewed journal publications and is in the editorial boards from *Frontiers in Chemistry Nanoscience*, *Industrial Lubrication and Tribology* as well as *Lubricants*. Furthermore, he is a member of the Society of Tribologists and Lubrication Engineers (STLE) and the German Society for Tribology (GfT).

Andreas Almqvist. He is a professor at the Division of Machine Elements, Luleå University of Technology (LTU), Sweden, where he leads the branch of research devoted to computational tribology. He is also currently acting as editor-in-chief for *Proceedings of the ImechE Part J—Journal of Engineering Tribology*. He has more than 100 publications and an H-index of 28. He has received a number of best paper awards and other academic prizes, and he is member of the editorial boards for *the Proceedings of the IMechE Part J—Journal of Engineering Tribology*, *Lubricants* (MDPI), *Fluids* (MDPI), and *Applications in Engineering Science* (Elsevier). He is also a Swedish Olympic Committee Research Fellow, conducting research in sports technology. In this role he is running a whole range of activities within the Ski- & Snow laboratory at LTU, in co-operation with the national teams in all disciplines of skiing. For more information about Andreas and his research, please visit his homepage: http://www.ltu.se/staff/a/almqvist.

Andreas Rosenkranz. He is a professor of materials-oriented tribology and new 2D materials in the Department of Chemical Engineering, Biotechnology and Materials at the University of Chile. His research focuses on the characterization, chemical functionalization, and application of new 2D materials. His main field of research is related to tribology (friction, wear, and energy efficiency), but he has also expanded his fields towards water purification, catalysis, and biological properties. He has published more than 100 peer-reviewed journal publications, is a fellow of the Alexander von Humboldt Foundation and acts as a scientific editor for different well-reputed scientific journals including *Applied Nanoscience* and *Frontiers of Chemistry*.

Michel Fillon. He is retired from CNRS and Pprime Institute, France, since January 2022. He has been a CNRS director of research at the Pprime Institute, University of Poitiers. From 2002 to 2010, he has been a manager of the "Lubricated Contact Mechanics" research group. His research interests were (still are) both experimental and theoretical investigations of hydrodynamic journal and thrust bearings. He is a fellow of ASME and STLE. From 2006 to 2008; he was the chair of Research Committee of ASME Tribology Division and from May 2016 to May 2021; he was a director of STLE Board of Directors. He was a member of the Annual Meeting Program Committee of STLE (from 2010 to 2018) and chair of the 73rd STLE Annual Meeting in May 2018 (Minneapolis); he has also organized nine EDF/Pprime Workshops on Journal and Thrust Bearings from the first one in 2002 to 2017. He has been co-editor-in-chief of *Tribology International* (from October 2014 to December 2021) and an associate editor of *ASME Journal of Tribology* (from 2003 to 2009). He is currently co-editor-in-chief of *Mechanics & Industry* and associate editor of *Lubricants* as well as editorial board member of several other journals.